The challenge of identifying and conserving valuable ecosystems close to human settlements in a northern area.

An approach based on field- and satellite data.

Ellen Margrethe Stabursvik

FACULTY OF SCIENCE
Department of Biology
University of Tromsø, N-9037 Tromsø
Autumn 2007

The best time to plant a tree was 20 years ago. The second best time is now.

~ Chinese Proverb

Master Thesis in Biology
Environmental Botany

The challenge of identifying and conserving valuable ecosystems close to human settlements in a northern area.
An approach based on field- and satellite data.

Ellen Margrethe Stabursvik
August, 2007

Norwegian Institute for Nature Research
Unit of Arctic Ecology
Polarmiljøsenteret
9296 Tromsø
Norway

Department of Biology
Faculty of Science
9037 Tromsø
Norway

Abstract

The rich broadleaved forests of North Norway have high species diversity. Mappings of biodiversity have been undertaken in the two municipalities Målselv and Bardu, but these mappings are far from exhaustive. This study examines classification methods for mapping rich broadleaved forests with the use of Landsat ETM+ images, and with vegetation indices as ancillary data. Three classifications were made; one supervised (on a July image) and two unsupervised (on the July image and a September image). Of these, the unsupervised classification of the July image had the best Overall Accuracy at 60.59 % and a Kappa coefficient of 0.4262. It seems that it is somewhat difficult to differentiate between the various rich broadleaved forest types with the use of Landsat ETM+ images, with their medium resolution, and a per-pixel classification. But with the added use of a tresholded NDVI it is possible to discern richer forest types in the study area, and to some degree imply what kind of forest we might expect to find based on the best classifications. I have compared my findings with the earlier biodiversity maps, and on this background I suggest that a new, and more thorough, mapping of the region is carried out.

1. Introduction

1.1 Background

Forests containing Aspen and Grey Alder are quite common in some parts of North Norway. Grey Alder is found in old forest pasture, at oxbow lakes and meandering rivers and other moist environments like ravines. When growing in hillsides it is usually on abandoned outfields characterized by reforestation (Naturforvaltning, 1999). Aspen grows from sea level to about 500 meters above sea level, and is usually found in mixture with other species, as single trees or grouped in small groves (Worrell, 1995). It is a very tolerant species regarding soil, temperature and moisture, and is found in different habitats. A lack of information on the growth extent and variation of these broadleaved forest types combined with a wish for more knowledge about them, constituted the background for this study. The two municipalities Målselv and Bardu hold large parts of these forest types in North Norway. Examinations of the biodiversity of Målselv and Bardu were undertaken by the Norwegian Institute for Nature Research (Norsk Institutt for Naturforskning, NINA) in 2000-2005 (Strann et al., 2005; Strann et al., 2005). The objective of this mapping was to designate areas of high biodiversity. In 1993, Norway ratified the Rio Convention on Biological Diversity from 1992. This convention commits the parties that ratify the convention to identify and conserve their biodiversity. It is important to conserve biodiversity because nature is of value in itself, and because of its usefulness to humans; it provides medicines, food, shelter, recreation and so on. Our environment is under increasing pressure from human influence; pollution, deforestation, desertification, global warming and the introduction of non-native species, to name but a few human induced threats to biodiversity. One requirement for protecting species is knowledge about them, which in turn requires, among other things, mapping. However, there are still several unmapped or poorly mapped regions in this area, as in most parts of Norway. Research undertaken in this study focus on rich and thermophilic deciduous forests. The objective is (a) to test different methods for locating high biodiversity areas using satellite images and geographic information system (GIS) software, and (b) to map areas with high biodiversity that have not previously been mapped in former biodiversity rapports.

> **Biodiversity** is defined as "the variability among living organisms from all sources, including, inter alia, terrestrial, marine, and other aquatic ecosystems, and the ecological complexes of which they are part: this includes diversity within species, between species and of ecosystems."
> *The Rio Convention, Article 2.*

The forests in Norway are very varied and usually have high species diversity. Almost half of the species on the Norwegian Red List lives in forests (State of the Environment Norway, 2006). Troms County is one of the counties with the highest share of deciduous forests in Norway. Rich, deciduous forests have a high species richness and the conservation of these forests is a special responsibility for Troms County (State of the Environment Norway, 2006). Nevertheless, these types of woods are traditionally looked upon as of little value in Norway, and have been treated accordingly. Deforestation, ditching, river straightening, planting of Norway spruce (*Picea abies*) and other human interferences have been imposed upon these forests, thus decreasing their extent and species richness. Still, there is an increasing awareness of the importance of conserving these particular types of biotopes, and in this respect, it is important to identify and record them to be able to protect them.

The production of land cover maps usually demands extensive fieldwork, but thorough fieldwork is usually too expensive, time consuming and personnel demanding to be implemented to a satisfying degree. With the use of satellite images and suitable methods in geographic information systems, large areas can be mapped on a preliminary basis with little or no ground truth data and thus imply areas of interest that should undergo more thorough examination. This is of course an advantage not only in issues of conservation, but also in land cover mapping with other goals in mind.

1.2 Objective

The objective is to apply methods that will enable us to map certain types of rich, deciduous forest by remotely sensed data. Using unsupervised and supervised classification on satellite images, the indices Normalized Difference Vegetation Index (NDVI), Normalized Difference Water Index (NDWI), a digital elevation model and ground truth data in a GIS, I tried to map these forest adequately, and then I compared them to the earlier maps on biodiversity produced by NINA. The purpose of this was to make a suggestion about areas which have not been surveyed earlier and that may be targeted for such biodiversity mapping.

The focus is on Grey Alder (*Alnus incana*) forest i.e. Grey Alder - Bird Cherry (*Prunus padus L*) forest and Aspen (*Populus tremula*) forests but also on Rich swamp woodland and rich birch woods (*Betula nana*), especially those growing on north-facing and moist hillsides and on higher altitudes. Grey Alder - Bird Cherry forests have a nutrient rich and moist environment, giving them high species richness in both plants and animals, and is in this respect a good candidate for protection (Naturforvaltning, 1999). In rich birch forests we will also find high biodiversity and production. Aspen forests are not usually mapped as a separate forest in Norway even though in the north of Norway Aspen can be found in large enough numbers or density to be to make up identifiable patches of forest. A significant feature of Aspen bark is its low acidity, which makes this nutritious bark an important substrate for lichen and moss (Street et al., 2001). Old Aspen forests are very species rich biotopes (Naturforvaltning, 1999). In addition to being poorly mapped in the study region, Aspen forests are important for biodiversity and hence interesting to this study of mapping methods.

2. Remote sensing: Theoretical background and methods

Remote sensing is based on techniques in which various sensors register reflected or emitted radiation from the earth or its atmosphere. Remote sensing observes a part or several parts of the electromagnetic spectrum, using sensors mounted on airborne (aircraft) or space borne platforms (satellites), thus enabling us to observe objects without disturbing them. (Sluiter et al., 2002). There are two types of remote sensing systems, passive and active. Passive systems, such as those onboard the Landsat satellites, observe reflected radiation from the ground. The energy source of this radiation is usually the sun. Active sensors, on the other hand, emit electromagnetic energy themselves and register the reflected radiation. Radars are typical active systems.

2.1 Landsat 7 ETM+

Remote sensing data for this study has been provided by the Landsat 7 ETM+ satellite sensor. The Landsat satellites have been active since 1972. These Earth-observing satellites are jointly managed by NASA and The U. S. Geological Survey (NASA, 2007). Landsat 7 was launched on April 15, 1999. The Earth observing instrument on Landsat 7, is the Enhanced Thematic Mapper Plus (ETM+) (NASA, 2007).

The tables presented in the following section are from the Australian Government Geoscience Australia (Acres, 2007). They have been somewhat altered to fit to the text.
The radiometric characteristics of Landsat 7 ETM+ sensor used in this study are presented in Table 1. Satellite and Image Characteristics of the Landsat 7 ETM+ are presented in Table 2.

2.2 The spatial resolution of the ETM+ sensors

The Landsat ETM+ data have a medium spatial resolution (30 m), which makes it quite easy to use ground truth data with the imagery. With lower resolution it would be a greater variation of vegetation type within pixels, and with an even higher resolution, for instance 1 meter, one tree might consist of several pixels that may be classified differently in a classification. Still, a typical Grey Alder - Bird Cherry forest is found along rivers and streams in thin bands, typically in often flooded areas. A 30 meter resolution might be to low for these particular bands of forests and give high interclass spectral variance, but it will probably detect larger areas of the riparian forests (Muller, 1997). Likewise, there may be a problem in identifying the Aspen, because they constitute quite small stands of forests.

Table 1. The radiometric characteristics of Landsat 7 ETM+ sensor.

Band Number	Spectral Range (in Microns)	EM Region	Generalized Application Details
1	0.45 - 0.52	Visible Blue	Coastal water mapping, differentiation of vegetation from soils and bare rock
2	0.52 - 0.60	Visible Green	Assessment of vegetation vigor
3	0.63 - 0.69	Visible Red	Chlorophyll absorption for vegetation differentiation
4	0.76 - 0.90	Near Infrared	Biomass surveys and delineation of water bodies
5	1.55 - 1.75	Middle Infrared	Vegetation and soil moisture measurements; differentiation between snow and cloud
6	10.40- 12.50	Thermal Infrared	Thermal mapping, soil moisture studies and plant heat stress measurement
7	2.08 - 2.35	Middle Infrared	Hydrothermal mapping
8	0.52 - 0.90 (panchromatic)	Green, Visible Red, Near Infrared	Large area mapping, urban change studies

Table 2. Satellite and Image Characteristics of the Landsat 7 ETM+ satellite.
* ETM+ band 8 (panchromatic) was designed to be acquired at 15m resolution, but post-launch testing shows a ground sampling interval closer to 18m.

Property		Landsat 7 ETM+
Ground Sampling Interval (GSI) (pixel size)	Bands 1-5 & 7 Band 6 Band 8	30 × 30 m 60 × 60 m 15 × 15 m pixel size (18 × 18m GSI)*
Swath width		185 km
Repeat coverage interval		16 days (233 orbits)
Altitude		705 km
Quantisation		Best 8 of 9 bits
On-board data storage		375 Gb (solid state)
Orbit type		Sun-synchronous
Inclination		98.2°
Equatorial Crossing		Descending node: 10:00am

2.3 Spectral characterization of vegetation

When sunlight strikes objects on the ground, certain wavelengths of the lights spectrum are absorbed and other wavelengths are reflected. Leaf cells scatter solar radiation in the near infrared region with wavelengths from 0.7 to 1.1 µm, and appear relatively bright in the near infrared band (NIR) and darker in the bands with visible light, because the chlorophyll in plants absorb light with wavelengths from 0.4 to 0.7 µm for use in photosynthesis. By contrast, clouds and snow tend to be rather bright in the red, as well as other visible wavelengths and quite dark in the near-infrared (NASA, 2007). The reflectance from vegetation measured by any remote sensing device is thus governed by the presence of absorbing pigments (i.e. chlorophyll) in the visible part of the spectrum (Figure 1), and by multiple internal reflections in the leaves of the plants in the near infrared part of the spectrum. In healthy vegetation, the latter produces typical high reflectance in the near infrared band (Rees, 1990).

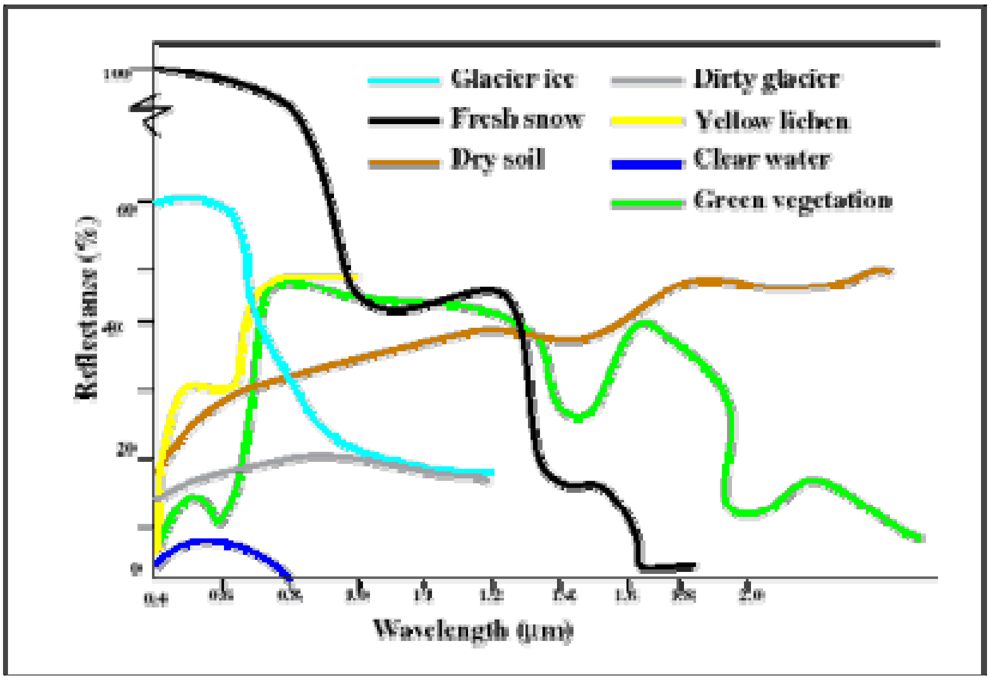

Figure 1. Spectral characterization of vegetation and other land cover units.

2.4 Classification

Classification of digital satellite data is the process in which the image pixels are being grouped into individual classes or categories based on their similarity in data values. Two methods of classification are commonly used: Unsupervised and Supervised Classification.

Unsupervised Classification uses various clustering algorithms to determine the natural spectral groupings within an image (Johnston, 1998). Erdas Imagine uses the ISODATA algorithm. ISODATA stands for "Iterative Self-Organizing Data Analysis Technique". This means that it repeatedly performs a classification and recalculates statistics, and then it locates the clusters that are inherent in the data. When the clustering is finished, the user must re-categorize these clusters into meaningful classes. (Leica Geosystems, 2006). In my thesis, I have used the Hyperclustering version of the Unsupervised Classification method.

Hyperclustering of multiband (multivariate) image data serves to segment the scene (landscape) according to prominent, spectral patterns of the environment (Myers et al., 1998). The number of such clusters is large, being chosen a priori to saturate the informational capacity of a byte of computer storage. Hyperclustering is informational advantageous for detecting changes from image datasets collected at different times over an area (Myers et al., 1998; Myers et al., 1999). It reduces the volume of data to be processed in change detection, and filters noise from conventional change indicators. The spatial segmentation further enables new kinds of change indicators, involving comparison of spatial organization between temporal image datasets. The spatial comparisons can be accomplished either by spectral averaging or spectral matching. The comparisons are temporally directional in the sense that going from earlier to later may reveal different aspects of change than retrospective comparison.

In **Supervised Classification**, the analysts trains the computer to recognize patterns in the data by selecting pixels that represents patterns or land cover features that she recognizes, or by using other sources of information like ground truth data, available maps or aerial photos. (Leica Geosystems, 2006). The signature files thus created are then used in the classification process where each pixel is categorized into the land cover class it mostly resembles. Products of this process being a thematic map, tables of statistics of the various land cover classes, and digital data files that can be included in a GIS. The classification itself is quite simple and is carried out by the software, the development of training sites requires much more effort. Ideally, all spectral classes constituting each information class should be represented in the training set statistics (Lillesand et al., 2000).

2.5 Vegetation indices

The satellite data were processed by extracting the NDVI and NDWI indices in order to detect areas with high biomass and high biodiversity.

Vegetation monitoring by vegetation indices

Vegetation Indices (VI) are techniques of multi-spectral transformation of satellite image data. They make use of the phenomenon, that different types of biomass reflect different amounts of energy in different bands. The reflectance characteristics in the red and the infrared bands have been used to monitor vegetation with remote sensing, and a range of different vegetation indices have been proposed in order to estimate the amount, productivity and health condition of the vegetation. Various mathematical combinations of spectral channels have been applied as sensitive indicators of the presence and condition of green vegetation (Justice et al., 1985; Tucker et al., 1986). Most simple of the vegetation indices is the vegetation index (VI), defined as "the ratio between the near-infrared channel and the red channel". The Normalised Difference Vegetation Index (NDVI) was found (Sellers, 1986; Tucker et al., 1986; Prince, 1991) to be a representative of plant assimilation condition and of its photosynthetic efficiency. NDVI is an indicator of the density of chlorophyll and leaf tissue calculated from the red and near infrared bands:

$$NDVI = (NIR - RED) / (NIR + RED)$$

Where NIR stands for the Near Infrared band 4 (0.76-0.90 μm) of Landsat 7 and RED is band 3 (0.63-0.69 μm). NDVI gives values between -1 and + 1. Vegetated areas in general yield high values for these indices due to their high near infrared reflectance and low visible reflectance. Reflectance for cloud, snow and water is larger in the red than near infrared. Clouds and snowfields yield negative values while water has very low or slightly negative values. Rock and bare soil have similar reflectance in red and near infrared channels, and results in indices near zero. A zero or close to zero means no vegetation. (Myneni et al., 1992; Slayback et al., 2003; Delbart et al., 2005).

Temporal changes in NDVI are related to the seasonal changes in the amount of photosynthetic tissues; typically NDVI increases in spring, saturates at a certain point of greenness in summer and then declines in autumn, at mid to high latitudes.

The NDVI equation has a simple, open loop structure. This renders the NDVI susceptible to large sources of error and uncertainty over variable atmospheric and soil background conditions, wetness, imaging geometry, and with changes within the canopy itself (Jackson et al., 1986; Sellers, 1986; Myneni et al., 1992). Several studies to improve the stability of the NDVI by correcting for soil and atmospheric sources of variance have been done. The NDVI and variants of NDVI like SAVI (Soil Adjusted Vegetation Index), SARVI (Soil Adjusted and Atmospherically Resistant Vegetation Index) and ARVI (Atmospherically Resistant Vegetation Index), are based on atmospheric models and are therefore limited in application in more wet areas, and therefore other vegetation indices have been established. Among them, NDWI (the Normalized Difference Water Index), for remote sensing of vegetation used in more wet terrain and for moist vegetation types (Gao, 1996), might be a good index in order to detect vegetation with high biodiversity in areas along rivers, mires and moist forests. The NDWI reminds of NDVI and is calculated for each pixel using the following formula:

$$NDWI = (NIR - SWIR) / (NIR + SWIR)$$

Where NIR is the Near Infrared band 4 (0.76-0.90 µm) of Landsat 7 and SWIR is the Short Wave Infrared band 5 (1.55-1.75 µm).

3. Study area and data

The area of study is the two municipalities Målselv and Bardu, situated in Troms County in Northern Norway. The region has a varied geography with a coastline, alpine mountains, deep valleys and rivers, farmland and forested areas with both conifers and broadleaved trees. The two valleys Målselvdalen and Bardudalen, with their rivers Målselva and Barduelva dominate this region. In between them there are alpine regions with mountains around 1700 meters (e.g. Nunjis at 1703 m and Kirkestind at 1681 m). Elevation in the study area ranged from 30 to 500 meters above sea level .There can be found a lot of glacial outwash and fluvial deposits in the region, and also rubble from landslides and bare rock covered with a thin layer of dirt (NGU, 2007). According to (Moen, 1998), this area falls into three vegetation zones: Middle Boreal, Northern Boreal and Low Alpine, and into the climatic zones O2, O1 and OC.
The two municipalities comprise approximately 6018 km^2 (where Målselv is the larger of the two with it's about 3321 km^2).

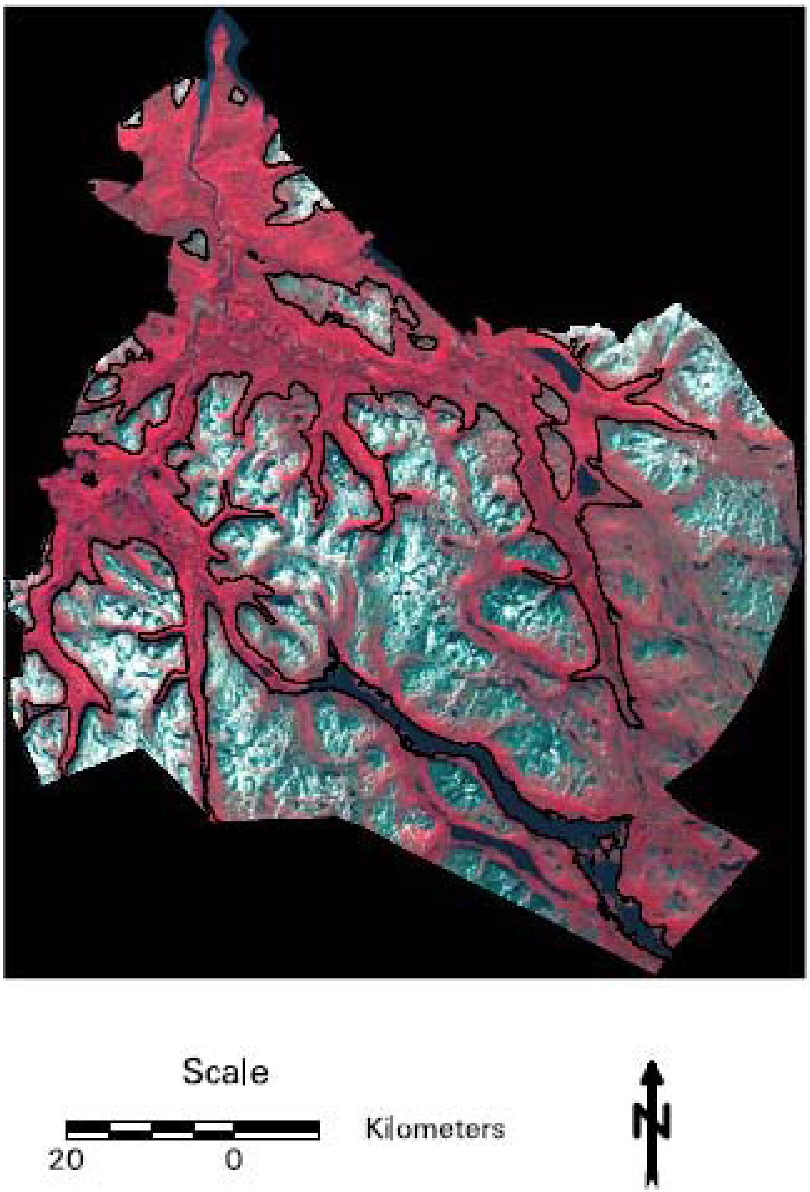

Figure 2. A Landsat ETM+ image showing the two municipalities Målselv and Bardu. The black line is the 500 meter above sea level limit for the study.

4. Data and methods

4.1 Remote sensing data

The Landsat 7 ETM+ data chosen for the project were taken on the 25th of July 2000. These multispectral images have originally a pixel-size of 30×30 meters, with a sun elevation of 40.4° and sun azimuth of 170.7°. An image from September 25th 1999, was also used. In addition, a Digital Elevation Model (DEM) over Troms County was utilised. This latter image has a pixel size of 25×25 meters.

4.2 Image processing and mosaicing

The GIS-software Erdas Imagine 9.1 from Leica geosystem was used to process the images. In order to cover the whole study area, two adjacent images where mosaiced together. The images had to be reprojected to the correct UTM zone 34 North using datum WGS 84. In this process, the pixel size was resampled to 25×25 meters to match the size of the DEM.
After merging the images together, the two municipalities Målselv and Bardu were cut out using map vector data (polygons) from The Norwegian Mapping Authority (Statens Kartverk). Only the forested regions are of interest in this project, and accordingly, all areas above the approximate timberline in this part of Norway, i.e. an elevation of 500 meters above sea level, were removed from the image. This was done by masking out the areas above 500 meters using the DEM which had previously been made into a binary image. Removing the mountainous regions might make the classifications more accurate, by lowering the number of possible classes that can be found by the classifier. It was desired to make a similar image for September, but unfortunately it was impossible to obtain images covering the whole area because of clouds on several of the images. The solution was to make a smaller image covering some interesting regions; like Devdislia in Dividalen, an area with old Aspen groves, and the area around the meandering Målselva, a rich alluvial plain. In autumn, the foliage of Downy birch is yellowish; that of Aspen is yellow to orange and Grey Alder retains its green leaves. The objective of making an autumn classification is to see whether these differences in autumn senescence will influence the classification. The mask made for the purpose of removing altitudes above 500 meters did not function on the smaller image, and as a consequence this image contains mountainous areas. This might influence the classification in several ways; one immediate effect was that it was necessary to make the vegetation classes a bit different for this image, as explained in the field work and vegetation data section.

Another fact to take into account concerning this image, is that sun is quite low on the horizon this far north in late September; consequently the image is somewhat marred by shadow-effects.

I used image offset to repair the slight distortion between the summer image and the autumn image. There was about 100-200 meters difference between the two. The September image lay a little bit northwest of the July image, probably because of unsatisfying orthorectification.

4.3 The classification process

Three different classifications were made; an unsupervised classification of the July image and one of the September image, and one supervised classification of the July image.
The signature file from the classifications were inspected in Signature Editor, an utility in Erdas Imagine that allows not only the making of spectral signatures in the supervised classification, but also evaluation of signatures from both supervised and unsupervised classification processes. In signature mean plots created in the Signature Editor, it is easy to compare the spectral responses of each signature class, in the different bands.

In order to reveal the spectral similarity between the obtained classes in the classified images, a dendrogram was constructed at the end of the classification procedure, using the **Dendrogram Tool** utility in Erdas Imagine. A dendrogram shows the spectral distances between classes in a hierarchical graphic (Leica Geosystems, 2006). The Distance Measure, a measure that finds the two classes that are nearest to each other, and join them into a new object, was set to Euclidean. The Agglomeration Method is then used to recompute the distance between the new object and the rest of the classes. The Agglomeration Method was set to complete linkage. See Appendix 2 for a dendrogram-example; the dendrogram from the unsupervised July classification.

In the first stages of **supervised classification,** a method of making vector polygons around ground truth data was used. This proved to be an unsatisfying method in that the polygons rarely obtained the desired shape and size and therefore produced areas containing heterogeneous pixel values, resulting in poor separation between different signatures. This in turn gave a map that was clearly poorly classified. Consequently, a method called **region**

grow tool was applied. In this process, a seed pixel is chosen, usually where a known ground control point is located. Then, pixels with similar spectral characteristics are included in the training site according to specified statistical parameters (Lillesand et al., 2000). The training signatures based on the exact pixel containing the gps point with the ground truth sample were made, using a geographic constraint of 300 pixels and a spectral Euclidean distance of 5. Upon inspection this immediately produced an improved classification. Still, several rounds of signature making and classifying processes remained before the classified image was visually satisfying. The classes resulting from the signatures were then inspected and aggregated into 9 classes and then 4 classes, as described chapter 5.1.1 and also in Appendix 4. Supervised classification was made only on the July image.

In the **unsupervised classification** approach, 75 spectral classes were generated. This is considered to be more like the hyperclustering approach presented in Chapter 2.4. The image was classified with a specified ISODATA convergence threshold of 0, 97. The 75 classes were then interpreted, labelled and aggregated into 9 classes and then 4 classes, as described chapter 5.1.2 and 5.1.3, and also in Appendix 4. Unsupervised classification was made on both the July and the September image.

After the classifications were completed a **Median filter** was run on the images. This is a spatial low pass filter, which outputs the median pixel value of the moving window of 3x3 pixels or larger. This method removes grainy noise from areas dominated by one class, while it preserves edges and fine structures like roads and rivers to some extent (Santos et al., 1998; Lillesand et al., 2000; Jensen, 2005). After filtering, new accuracy assessments were made on the images.

Because the accuracies of the different classes varied greatly between the classifications the best of the four rich broadleaved forest classes were extracted from the classification where they had the highest accuracy, and then utilized in vegetation maps. This way, the final results contains elements from all the classifications.

4.4 Fieldwork and vegetation data

The satellite images were taken in the autumn of 1999 and the summer of 2000, while the field work was undertaken about six years later during the summer months of 2006. This is not an ideal situation and may give some inconsistencies between these two data types. Ideally, field work and the images should be from about the same period of time so that the data correspond as much as possible.

Fieldwork was undertaken in three turns; a short trip to Dividalen in the beginning of September 2005, two weeks in June and July 2006, and finally a week in the middle of September 2006. The field data was sampled for use as ground truth data for training in the classification process and for use in accuracy assessment.

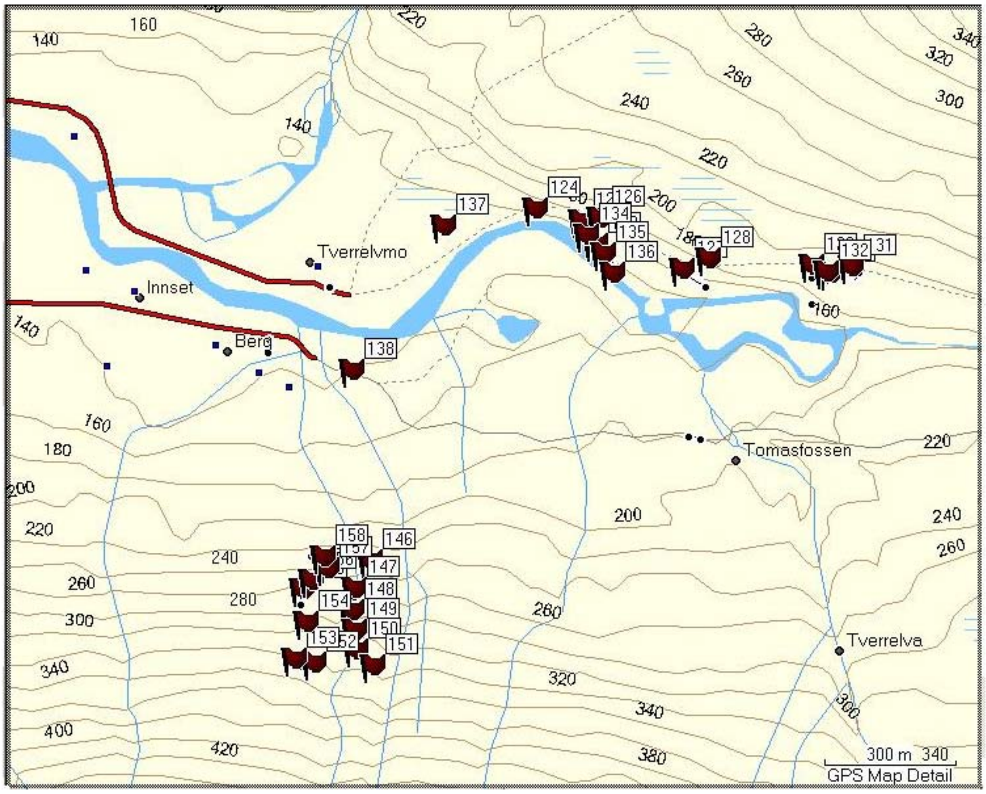

Figure 3. Segment of map from Garmin's MapSource showing examples of ground control points

The areas of interest were not chosen randomly, but based on prior knowledge of the area and with the intention of finding areas complementary to already mapped areas. This knowledge came from different sources; Biodiversity reports (Strann et al., 2005; Strann et al., 2005), other Master Thesis (Larsen, 2004), local knowledge etc. This was done because the study area is too big to cover properly with random sampling, and because time and economy were limiting factors. Within the chosen areas, plots were randomly selected. Most plots were taken in the vegetation types that were relevant to the project, mainly rich, broadleaved forests. Several plots are from other types as well, for use in supervised classification. Each plot represents a point, i.e. the vegetation type in the immediate area of the gps point. The gps used was a Garmin eTrex. Examples are shown in Figure 3. Registrations in each plot were simple since major forest types was the main concern. Minor variations in the forest floor vegetation will not show up in the satellite images. Plants were recorded using a 1-5 system, the Braun-Blanquet scale; where 1 indicates a rare species in that plot and 5 denotes a dominant species in the plot.

The nomenclature of the plants is according to Lid's Norske Flora (Lid et al., 2005). See Appendix 1 for a list of species encountered in the field. The English names are taken from (Anderberg et al., 2007).

Initially, the vegetation data were classified using the TWINSPAN software and this grouping of the Ground Control Points (GCPs) were used in the classification of satellite data. Upon inspection of the classified vegetation data, it became evident that the TWINSPAN classification was unsuitable for this purpose; several samples without Grey Alder were put in the Grey Alder class, and samples lacking in Downy Birch were put in groups with birch and so forth. The problem was solved by taking a more subjective approach, where the Twinspan classification was used as a guideline in the grouping of the samples according to field notes, and the classification system of Eli Fremstad in "Norwegian vegetation types" (Fremstad, 1997). The classes used are also according to Fremstad's system. See Appendix 3 for a description of the forest types under study, and abbreviations used henceforth for simplicity. In addition to the ground truth data mentioned, other sources of data were employed. These were field data from another master thesis studying the same area (Werth, 2001), a report made by NINA from the Målselv estuary (Systad et al., 2000) and a vegetation map covering a part of Bardu (NIJOS, 1991).

4.5 Classification assessment of vegetation maps

Accuracy of maps based on remotely sensed data can be divided into positional and thematic accuracy. Positional accuracy refers to the accuracy of a geometrically rectified image. The positional error of the final product is below the grid cell size (25 m) and can therefore be ignored. Thematic accuracy refers to the non-positional characteristics (attributes) of spatial data (Janssen et al., 1994), in this case the vegetation cover unit for a particular grid cell. The assessments of the accuracy of vegetation maps produced in my study were done by the site-specific method (Van Genderen, 1978; Reichert et al., 1984), comparing the satellite data based vegetation cover map to ground control points observed in the field, and for the non-rich broadleaves classes, points extracted from the vegetation map of parts of Bardu municipality produced by The Norwegian Forest and Landscape Institute (NIJOS, 1991)

The available vegetation data was divided into two groups; one for use in the classification process, and one for the accuracy assessment (validation) of the classification (Congalton, 2004). Two or more plots used in the validation of the land cover maps should not fall into the same pixel, because of this, points collected in the field were filtered so that no points for use in accuracy assessment are closer than 30 meters. Redundant points were then used in the supervised classification. When extracting points from the vegetation map using the GIS-software ArcView, parameters were set to avoid the points falling into the same pixel and to make sure they were at least 30 meters from the border of the polygon. More plots were kept for use in validation than for the classification. According to Lillesand and Kiefer (Lillesand et al., 2000), it is not unusual to have 100 or more training sites to adequately represent the spectral variability in an image. With about 250 collected ground control points and over 100 used in training, Congalton's (Congalton, 2004) advise of a minimum of 50 samples for each land cover category could not be attained for most classes. The 50 samples limit is considered to be statistically sound and also attainable. Unfortunately, time was limited and fewer ground control points were sampled for validation. Also, according to Congalton, it may be useful to concentrate on the land cover types of interest, in this case, to have more samples taken in rich, broadleaved forests and fewer in the other classes. I have used the vegetation map of parts of Bardu (NIJOS, 1991) to collect points for use in the assessment of the other classes and my collected samples for the rich broadleaves forests.

The total accuracy of the classified images was calculated in an error matrix produced by the accuracy assessment utility in Erdas Imagine. This utility produces an Error Matrix, Accuracy Totals and Kappa statistics. Total accuracy is computed by dividing the total correct, by the total sum of sample units in the error matrix. The errors of omission or producer's accuracy, so called because the producer of the classification is interested in how well a certain area can be classified, is calculated. This is obtained when the total number of correct sample units in a category is divided by the total number of reference samples from that particular category. Commission or user's accuracy is a measure of reliability, and shows the probability of a sample unit classified on the map is the same category on the ground.

4.5.1 The significance of the classification accuracy assessments - The Kappa value

The Kappa value (index) is an accuracy statistic that represents the proportion of agreement obtained after removing the proportion of agreement that could be expected to occur by chance. It allows to test if a classification result is significantly better than if the map had been generated by randomly assigning labels to areas (Congalton, 2004). The Kappa value is widely used because all elements in the classification error matrix, and not just the main diagonal, contribute to its calculation, and because it compensates for change agreement. The Kappa coefficient lies typically on a scale between 0 and 1, where the latter indicates complete agreement, and is often multiplied by 100 to give a percentage measure of classification accuracy. Kappa values are also characterized into 3 groupings: a value greater than 0.80 (80%) represents strong agreement, a value between 0.40 and 0.80 (40 to 80%) represents moderate agreement, and a value below 0.40 (40%) represents poor agreement (Congalton, 2004). However, it should be noted that the level of accuracy sought and obtained in remote sensing projects depend on the level of classification employed, the scale of the area considered in the study as well as the spatial resolution of the imagery utilized in the analysis. In praxis, the Kappa value favours an uneven distribution of misclassified pixels, because it is less random. On the other hand, a classifier with a strongly skewed distribution seems not to be optimized.

4.6 Vegetation indices

Both an NDVI and an NDWI image of the study area were produced to be used as ancillary data in the process of identifying places with high biodiversity.

The NDWI image displayed a high susceptibility to striping effects in the original multispectral image. Because of this, it was rejected for purposes of identifying biodiversity. It is a good example of striping effects in satellite images though, and the problems this may cause. In Figure 4, there are two stripes: one stripe from the mosaicing of the two images constituting the study area (marked with blue crosshairs) and one stripe inherent in the images, probably as a consequence of some defect in the satellite (marked with red crosshairs). These stripes are also present in the original multispectral image, although not as evident. These stripes could mean that there are spectral differences in the image because of matters relating to the sensors aboard the satellites. These irregularities may influence the classifications and indices.

The NDVI was given a 0.6 threshold, by using a simple model (Figure 25 in Appendix 5). This means that the image was made into a Boolean image where all values above 0.6 were set to one and the rest as zero. The value of 0.6 was chosen after areas known to have high species richness were examined for their NDVI values. Afterwards, the threshold image was used to make a new vector image where both NDVI above 0.6 and rich broadleaved forest types were present. This was made using the model in Figure 26 in Appendix 5, and the unsupervised July classification. The result is presented in chapter 5.4.

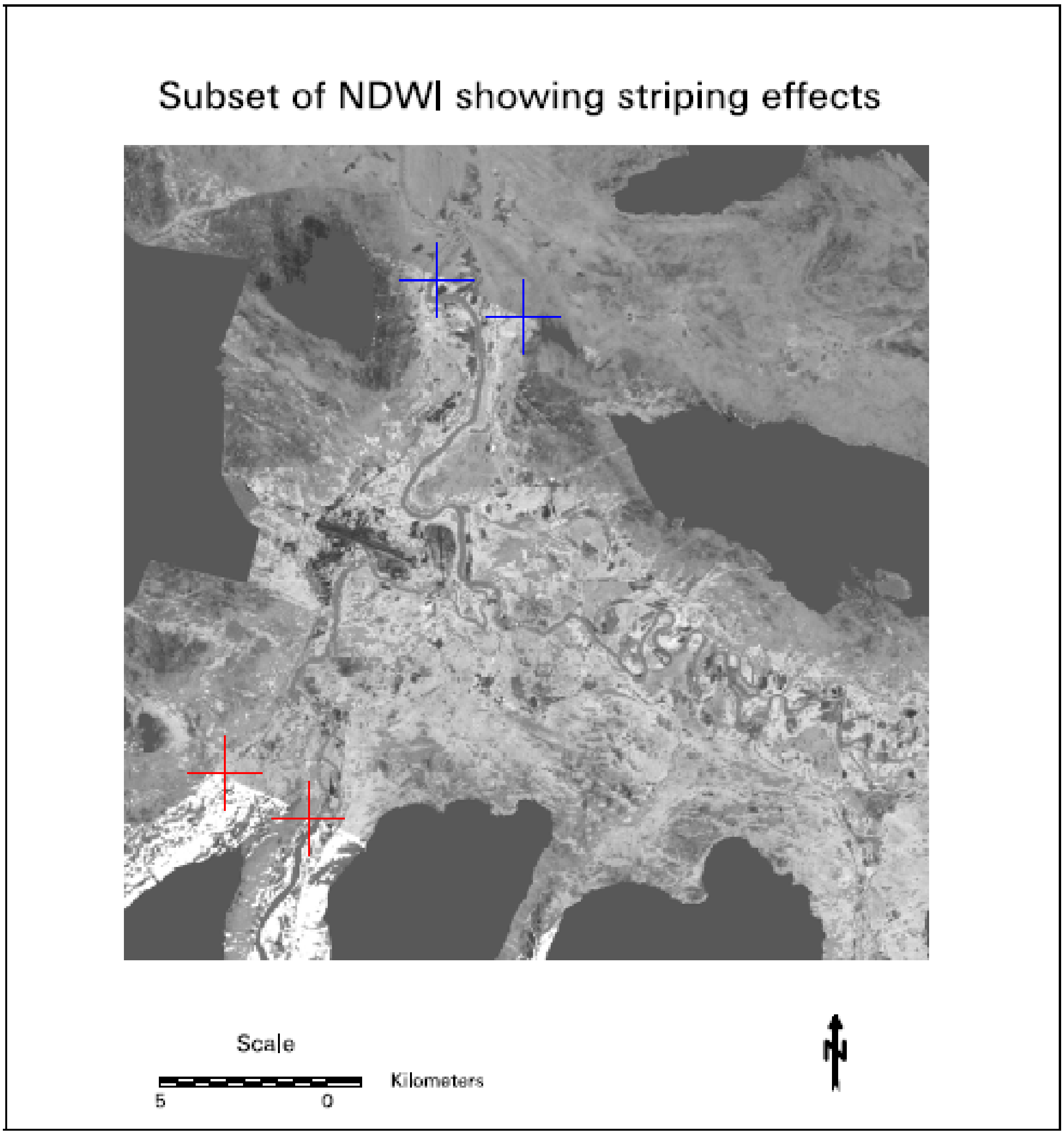

Figure 4. An NDWI that clearly displays the striping effects in the imagery. Blue crosshairs indicates the seam between the two images that where mosaiced, the red crosshair indicates a stripe in the image that probably originates from the sensor aboard the Landsat 7 satellite.

5 Results

5.1 Classifications

Three different satellite data classifications were made: one supervised and one unsupervised of the July image, plus an unsupervised one of a subset of the September image. Presented in this section, are the final products, together with some of the steps leading up to them (Figure 5 – 18 and Table 3 – 14). Appendix 4 presents the intermediate steps in the classification process (Table 16 – 30). The dendrogram from the unsupervised July classification is presented in Appendix 2.

5.1.1 Supervised classification of the July image

The first supervised classification was made with 11 classes, attempting to differentiate between fern and herb dominated Grey Alder forests, and Rich swamp woodland. See Appendix 4 for the accuracy assessment report from this classification (Tables 16 and 18). This first run had an overall accuracy of only 41.91%, and a Kappa coefficient of 0.3079.

In Figure 5, a plot shows spectral signatures from the three different Grey Alder forest types, collected from signatures where there were known ground control points. The signatures named “Alder river/hillsides” have been extracted from another Master thesis (Werth, 2001), and are probably containing both fern and herbs. This plot implies strong similarities between the fern (*Matteuccia struthiopteris*) dominated and the herb dominated Grey Alder types, even though the fern-type seems to have a somewhat higher reflectance in band 5, compared to that of the herb-variety. Also, the accuracy of the two classes is very low and the number of samples is below the ideal number of at least 50 per class (Congalton and Green, 1999).

It is also evident that Rich swamp woodland was not well classified at all, with an accuracy of zero. This might imply that this woodland is difficult to separate, with medium spatial resolution (e.g. Landsat ETM+ images), from the quite floristically similar Grey Alder classes. Figure 6 is a signature mean plot of Rich swamp woodland, together with signatures from the Grey Alder classes. This plot implies that the spectral responses of the classes are quite similar. A study made by Larsen (Larsen, 2004) in the same area as this study, indicates that the Landsat imagery used does not have a satisfactory spatial resolution for mapping these subtypes of middle boreal alluvial forest. Based on these facts, the three classes were merged in an attempt to attain better accuracy.

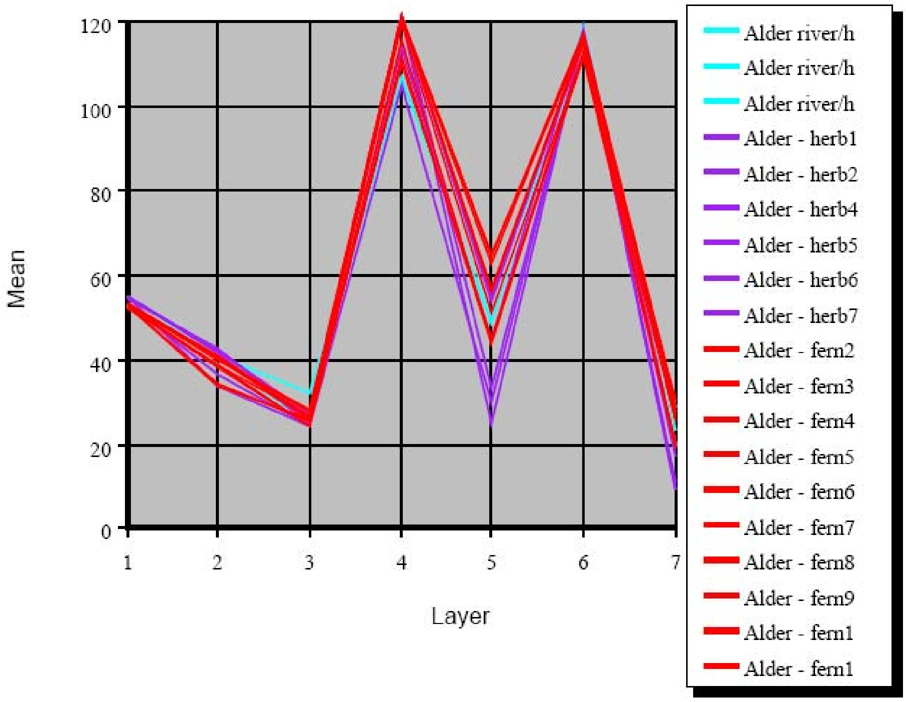

Figure 5. Signature mean plot showing the three types of ground control Grey Alder forests used in the supervised classification

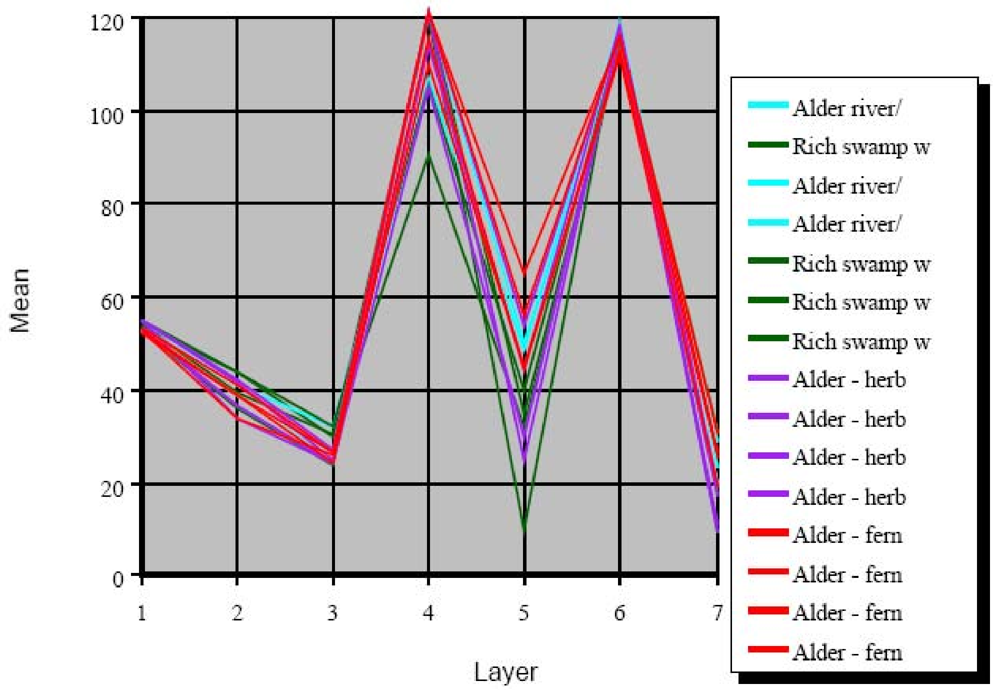

Figure 6. Signature mean plot. Fern and herb dominated Grey Alder forest, and Rich swamp woodland.

Plotting the signatures of the different classes of Aspen, Figure 7, against the Tall herb classes, it looks like they are too similar spectrally to distinguish from each other when using this supervised classification on Landsat images. Still, trying to determine the location of Aspen stands in the study area is one of the major objectives of this study, and the class will be kept.

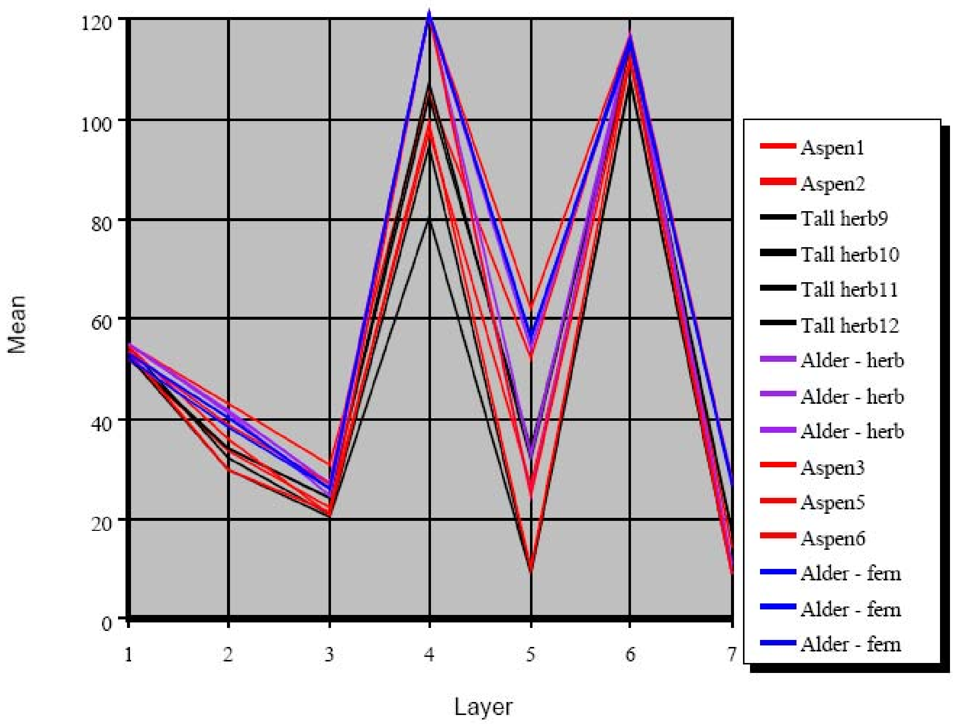

Figure 7. Signature mean plot showing signatures from Aspen, Grey Alder and Tall herb

Due to the findings mentioned above, a supervised classification was made in which the class Rich swamp woodland was merged with the class Grey Alder forest. In this classification the classes: 1 Grey Alder, 2 Aspen, 3 Tall herb, 4 Low herb, 5 Lichen/bryophyte, 6 Meadow/mire/heath, 7 Agriculture/ open field, 8 Urban and 9 Water, are present. This classification gave an overall accuracy of 43.23% and a Kappa Coefficient of 0.3360, when using the following class value assignment options; Clear majority, Discard window and Window size 3 (Table 20 and 21).

This classification was the best of several attempts. It was then recoded so that all other classes except the rich broadleaves were set to zero. Accuracy assessments were made of this image and are presented in Table 3 – 5.
There were no improvements after a Median filter had been used on the image.

Table 3. Accuracy totals of the July supervised classification. Class 0 is unclassified, 1 is Grey Alder, 2 is Aspen, 3 is Tall herb, 4 is Low herb. Ref. tot is total number of ground truth points for that class, Class.tot. is classified totals, Nr. corr. is number correct, Prod. acc. is producers accuracy and Users acc. is users accuracy.

Class Name	Ref. Tot	Class. Tot.	Nr. Corr.	Prod. Acc.	Users Acc.
Class 0	169	148	129	---	---
Class 1	78	23	14	17.95%	60.87%
Class 2	19	20	7	36.84%	35.00%
Class 3	25	71	12	48.00%	16.90%
Class 4	15	45	8	53.33%	17.78%
Overall Classification Accuracy =	55.37%				

Table 4 . Accurcay assessment error matrix of the supervised July classification**.** Background is unclassified, 1 is Grey Alder, 2 is Aspen., 3 is Tall herb, 4 is Low herb.

	Reference Data				
Classified Data	Background	Class 1	Class 2	Class 3	Class 4
Background	129	14	2	2	1
Class 1	3	14	1	4	0
Class 2	0	9	7	4	0
Class 3	17	29	7	12	6
Class 4	20	12	2	3	8

Table 5. Kappa statistics of the supervised July classification. Class 0 is unclassified, 1 is Grey Alder, 2 is Aspen, 3 is Tall herb, 4 is Low herb.

Conditional Kappa for each Category.	
Class Name	Kappa
Class 0	0.7144
Class 1	0.4754
Class 2	0.3071
Class 3	0.0953
Class 4	0.1355
Overall Kappa Statistics = 0.3491	

The results from the supervised classification accuracy assessment show an overall classification accuracy of 55.37 % (Table 3). The Kappa coefficient is 0.3491 (Table 5).

5.1.2 Unsupervised classification of the July image

Upon inspection of the signatures (Figure 8) of fern dominated and herb dominated Grey Alder forests, I found that these two classes may be hard to distinguish from each other (as shown in the supervised classification as well), and the two classes were merged before recoding of the image. Rich swamp woodland was also put in this class, because of its spectral similarity with Grey Alder forests (Figure 9), and because of the minimal number GCP for accuracy assessment in this class.

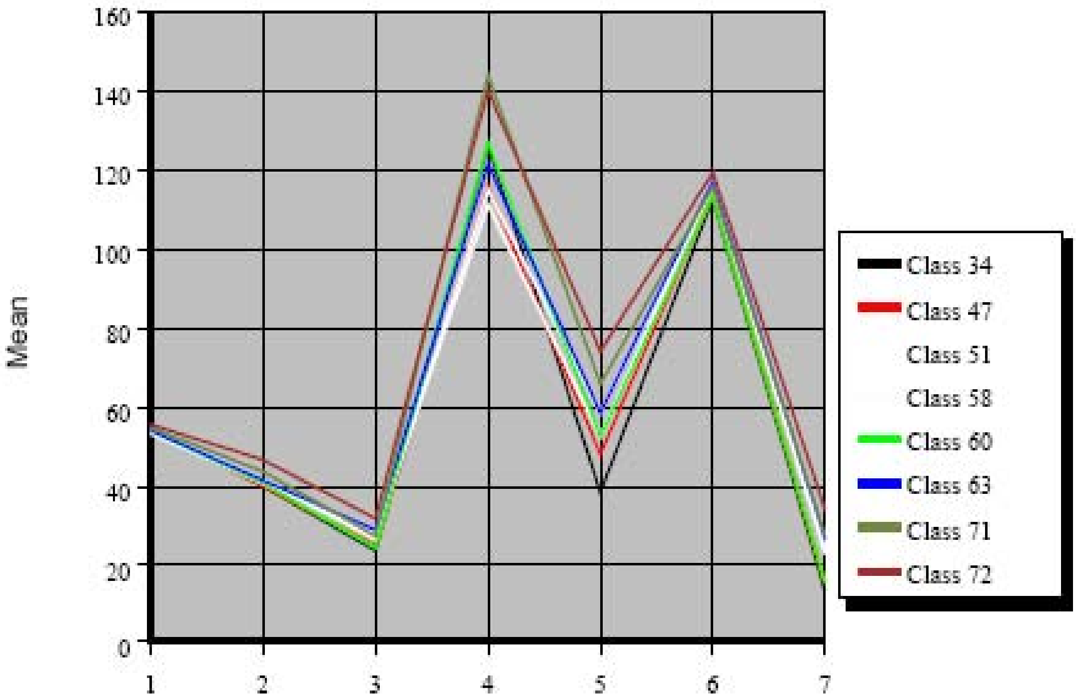

Figure 8. Grey Alder forest**.** Colored are fern, white are grass/herb

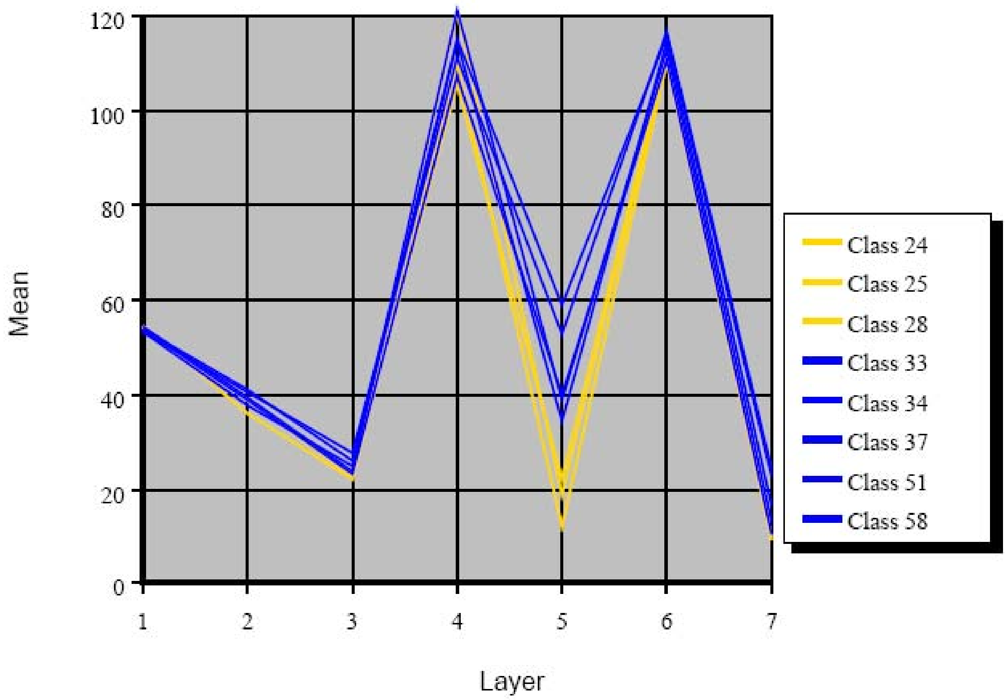

Figure 9. Signature mean plot showing swamp woodland in yellow (classes 24, 25 and 28) and Alder forest in blue (classes 33, 34, 37, 51 and 58).

Figure 10 is a signature mean plot that shows the different signatures from the rich, broadleaved forests together.

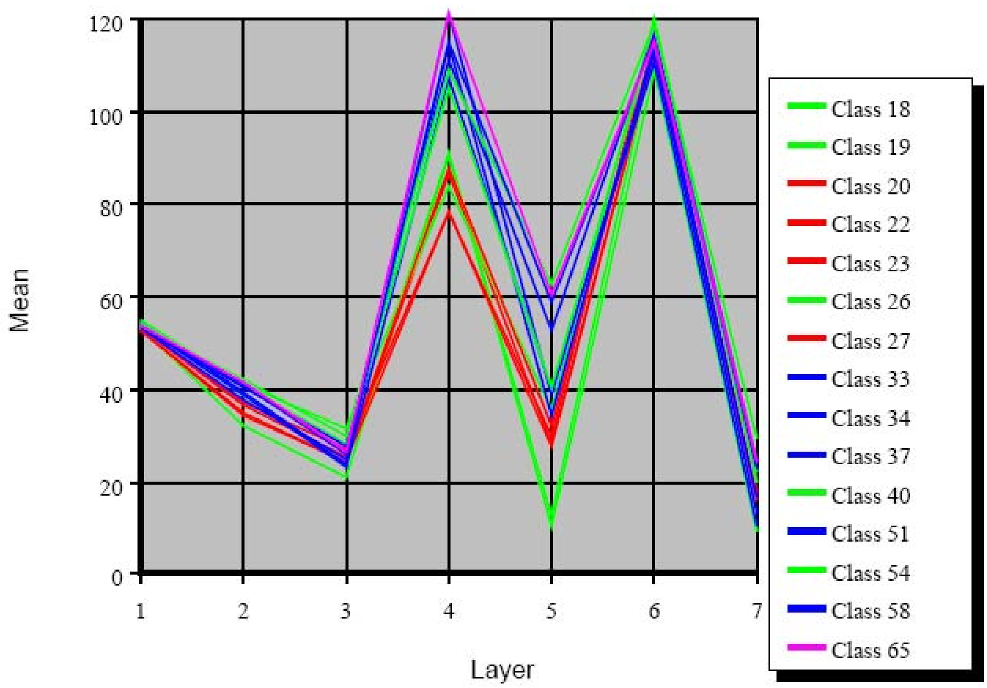

Figure 10. Signature mean plot**.** Aspen is shown in pink (class 65). Alder is in blue (33, 34, 37, 51, and 58). Tall herb is in green (18, 19, 26, 40, 54) and Low herb is in red (20, 22, 23 and 27).

The accuracy results of this classification are 48.83 % Overall Accuracy and a Kappa coefficient of 0.3859, when using the following class value assignment options; Clear majority, Discard window and Window size 3. This classification was made with nine classes, and the results are displayed in Appendix 4 (Tables 22 – 27).

This classification was the best of several attempts. It was then Recoded so that all other classes except the rich broadleaves was set to zero. An accuracy assessment was made of this image and is presented in Table 6 – 8.
There were no improvements after a Median filter had been used on the image.

Table 6. Accuracy totals of the July unsupervised classification. Class 0 is unclassified, 1 is Grey Alder, 2 is Aspen, 3 is Tall herb, 4 is Low herb. Ref. tot is total number of ground truth points for that class, Class. tot. is classified totals, Nr. corr. is number correct, Prod. acc. is producers accuracy and Users acc. is users accuracy.

Class Name	Ref. tot.	Class. Tot.	Nr. Tot.	Prod. Acc.	Users Acc.
Class 0	169	119	107	---	---
Class 1	78	94	54	69.23%	57.45%
Class 2	19	12	6	31.58%	50.00%
Class 3	25	61	10	40.00%	16.39%
Class 4	15	21	9	60.00%	42.86%
Overall Classification Accuracy = 60.59%					

Table 7. Accuracy assessment, error matrix of the unsupervised July classification. Background is unclassified, 1 is Grey Alder, 2 is Aspen., 3 is Tall herb, 4 is Low herb.

	Reference Data				
Classified Data	Background	Class 1	Class 2	Class 3	Class 4
Background	107	8	1	2	1
Class 1	16	54	7	12	5
Class 2	1	4	6	1	0
Class 3	33	12	5	10	0
Class 4	12	0	0	0	9

Table 8 Kappa statistics from the July unsupervised image. Class 0 is unclassified, 1 is Grey Alder, 2 is Aspen, 3 is Tall herb and 4 is Low herb

Conditional Kappa for each Category.	
Class Name	Kappa
Class 0	0.7757
Class 1	0.4295
Class 2	0.4670
Class 3	0.0898
Class 4	0.3992
Overall Kappa Statistics = 0.4262	

The accuracy assessment of the unsupervised July classifications shows an overall classification accuracy of 60.59% (Table 6). The Kappa coefficient is 0.4262 (Table 8). The dendrogram from this classification is displayed in Appendix 2.

5.1.3 Unsupervised classification of the September image

Because of problems with the autumn satellite images, classes in the initial classifications were slightly different from the others. Clouds and haze in the original Landsat images made it necessary to make a subset of just one of the images. As a result, the 500 meter mask made for the whole area did not work, and the subset has mountainous areas. In the process of recoding the original 75 classes for this classification, classes containing mountain, snow and shadow were set to zero, giving an image with unclassified areas below 500 meters and classified areas above 500 meters (especially class 6; Meadow). Because this was a subset of the original image, there are fewer ground control points for assigning clusters to classes and for accuracy assessment. Accordingly; there are greater uncertainties in both the assigning of classes in the classification, and in the accuracy assessment, than we will find in the other classifications. See Appendix 4 (Table 28-30) for results of this 9-class classification.

There are some major problems in identifying Low herb forest in this late September image. Some of the reasons for this may be that some of the places with this vegetation type have fallen in shadow; several of the ground control points for this forest type were in shadowed areas.

Figure 11 shows the variety of signatures from the classification.

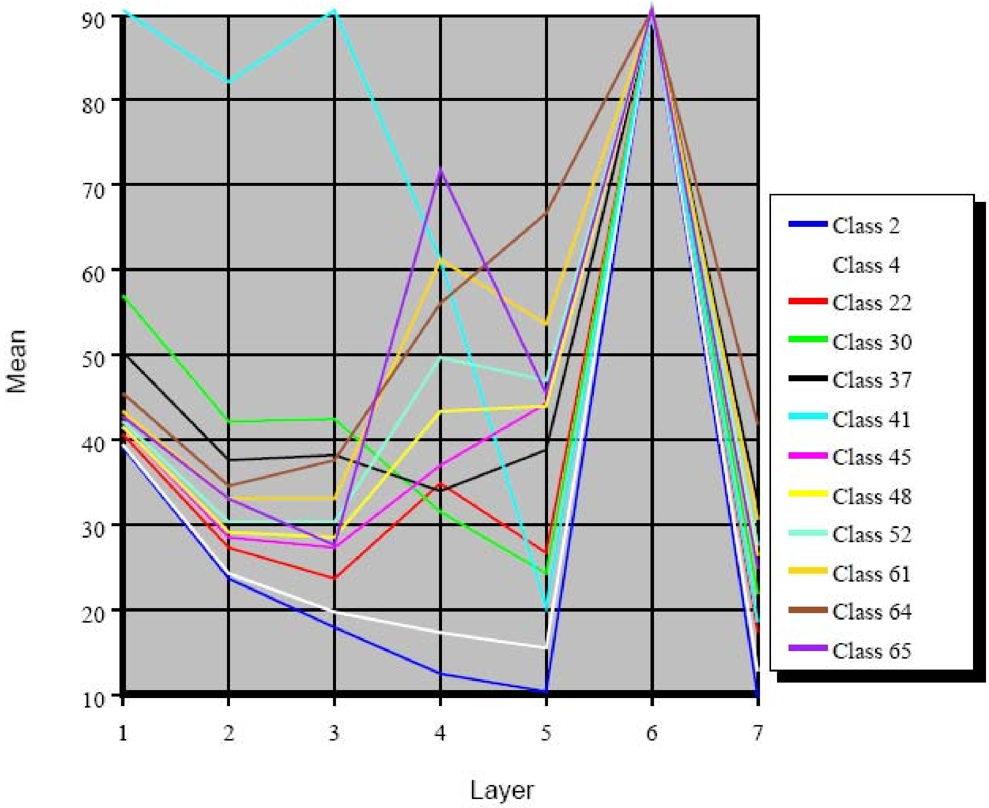

Figure 11. Signature mean plot, all classes – September**.** Class 2 water, 4 Shadow, 22 Lichen/bryophyte, 30 Mountain, 37 Urban/bare rock, 41 Snow, 45 Tall herb, 48 Aspen, 52 Grey Alder, 61 Low herb, 64 Meadow/mire/heath, 65 Agriculture/open field.

One of the intentions of making a September image was to check if it is easier to discern Grey Alder forest from Tall herb forest. This is because Grey Alder stays green until the leaves fall in autumn. It seems, from the accuracy assessments, that both Grey Alder forest and Aspen forests are a little easier to discern on the September image. Aspen has an early senescence and turns early, before the leaves fall.

Figure 12 present a signature mean plot where Grey Alder forest and Tall herb forest are displayed together.

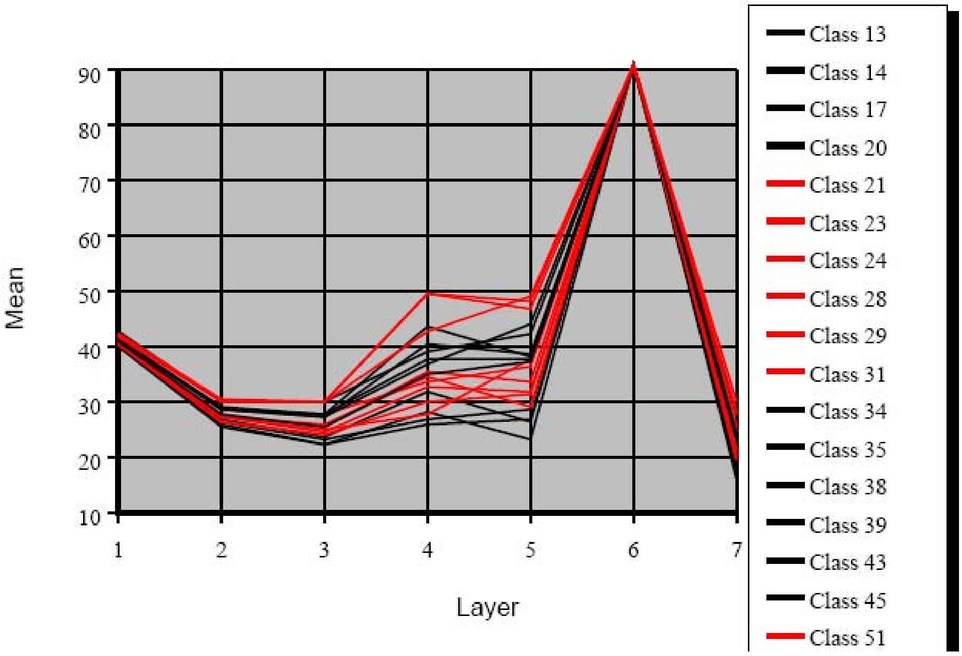

Figure 12. Signature mean plot. Alder is shown in red, Tall herb in black

An accuracy assessment was run on the resulting 9-class image, using these class value assignment options; Majority Threshold 9, Use Center Value and Window size 3. This classification had an overall accuracy of 46.28 % (Table 29) and a Kappa coefficient of 0.3254 (Table 30).

This classification was recoded, all classes except the rich broadleaves were set to zero, and an accuracy assessment was made of this image, and is presented in Table 9 – 11.
After running a Median filter on this classification, the accuracy stayed the same.

Table 9. Accuracy totals of the September unsupervised classification. Class 0 is unclassified, 1 is Grey Alder, 2 is Aspen, 3 is Tall herb, 4 is Low herb. Ref. tot is total number of ground truth points for that class, Class..tot. is classified totals, Nr. corr. is number correct, Prod. acc. is producers accuracy and Users acc. is users accuracy

Class Name	Ref. Tot.	Class. Tot.	Nr. Corr	Prod. Acc.	Users Acc.
Class 0	48	44	33	---	---
Class 1	41	32	21	51.22%	65.63%
Class 2	11	7	4	36.36%	57.14%
Class 3	15	36	6	40.00%	16.67%
Class 4	6	2	0	0.00%	0.00%
Overall Classification Accuracy =	52.89%				

Table 10. Accuracy assessment error matrix of the unsupervised September classification. Background is unclassified, 1 is Grey Alder, 2 is Aspen., 3 is Tall herb, 4 is Low herb.

	Reference Data				
Classified Data	Background	Class 1	Class 2	Class 3	Class 4
Background	33	8	0	3	0
Class 1	4	21	0	5	2
Class 2	0	2	4	1	0
Class 3	10	10	6	6	4
Class 4	1	0	1	0	0

Table 11. Kappa statistics from the September unsupervised image. Class 0 is unclassified, 1 is Grey Alder, 2 is Aspen, 3 is Tall herb and 4 is Low herb.

Conditional Kappa for each Category.	
Class Name	Kappa
Class 0	0.5856
Class 1	0.4801
Class 2	0.5286
Class 3	0.0487
Class 4	-0.0522
Overall Kappa Statistics = 0.3486	

The results from the accuracy assessment of the unsupervised classification of the September image show an overall accuracy of 52.89 % (Table 9). The Kappa coefficient is 0.3486 (Table 11)

5.2 Key results of the classifications

It seems that the different classifications function a little differently on the classes. Table 12 lists the Users Accuracy for each class, and Table 13 lists the area each class covers in the different classifications. The overall best accuracy is shown in bold. The unsupervised September image is the best for discerning Aspen and Grey Alder forests, but since this is a subset with few GCP for accuracy assessment, the results are shown in brackets and the second best results are shown in bold as well. Low herb appears to be best classified in the unsupervised July image. As we can see, the Tall herb class has a very poor accuracy. This might be a consequence of the inherent spectral similarity Tall herb, Downy Birch forests have to Grey Alder forests.

Table 12. Table is showing Users Accuracy from the different classifications. The best Users accuracy (comission) for each class is shown in bold.

Users Accuracy			
Class	Unsupervised, July	Supervised July	Unsupervised, September
Class 1	57.45 %	**60.87 %**	**(65,63 %)**
Class 2	50.00 %	**50 %**	**(57.14 %)**
Class 3	16.39 %	**16.90 %**	16.67 %
Class 4	**42,86 %**	17.78 %	0 %

Table 13. Area, in km^2, for each rich broadleaved forest type, from each classification

Area in km^2			
Class	Unsupervised, July	Supervised, July	Unsupervised, September
Class 1	348	**66**	**149**
Class 2	37	**97**	**39**
Class 3	508	**268**	231
Class 4	**129**	396	86

To better visualize the difference in the two classifications covering the whole study area (the July classifications), the area each land cover type covers in the classifications, is presented in Table 14.

Table 14. Land cover area for the 9-class classifications of the July image.

Class	Area in km^2 Supervised	Area in km^2 Unsupervised
Unclassified	9088	9098
Grey Alder – Bird cherry forest	**66**	348
Aspen	**97**	37
Tall herb, Downy birch forest	**268**	508
Low herb, Downy birch with scattered tall herbs	396	**129**
Lichen/bryophyte and dwarf scrub woodland	645	297
Meadow/bog/heath	41	173
Agriculture/open fields	0.063	106
Urban	156	50
Water	225	236

Each of the best classes in Table 12 were extracted from the classification with the best result for that class, and turned in to a shapefile. Each class is then presented with the Biodiversity Maps for the two municipalities in the 5.3 Vegetation Maps section.

5.3 Vegetation maps

The different vegetation maps are presented in Figure 13 – 18. Each map presents the boundary of the study area in red, the turquoise polygons are the previously mapped Biodiversity areas (Strann et al., 2005; Strann et al., 2005), and the green polygons symbolizes a forest type. Before vectorizing the raster images of the single-class images, a 3x3 Median filter was run to remove some of the “salt- and pepper-effect” thus making the images more viewable.

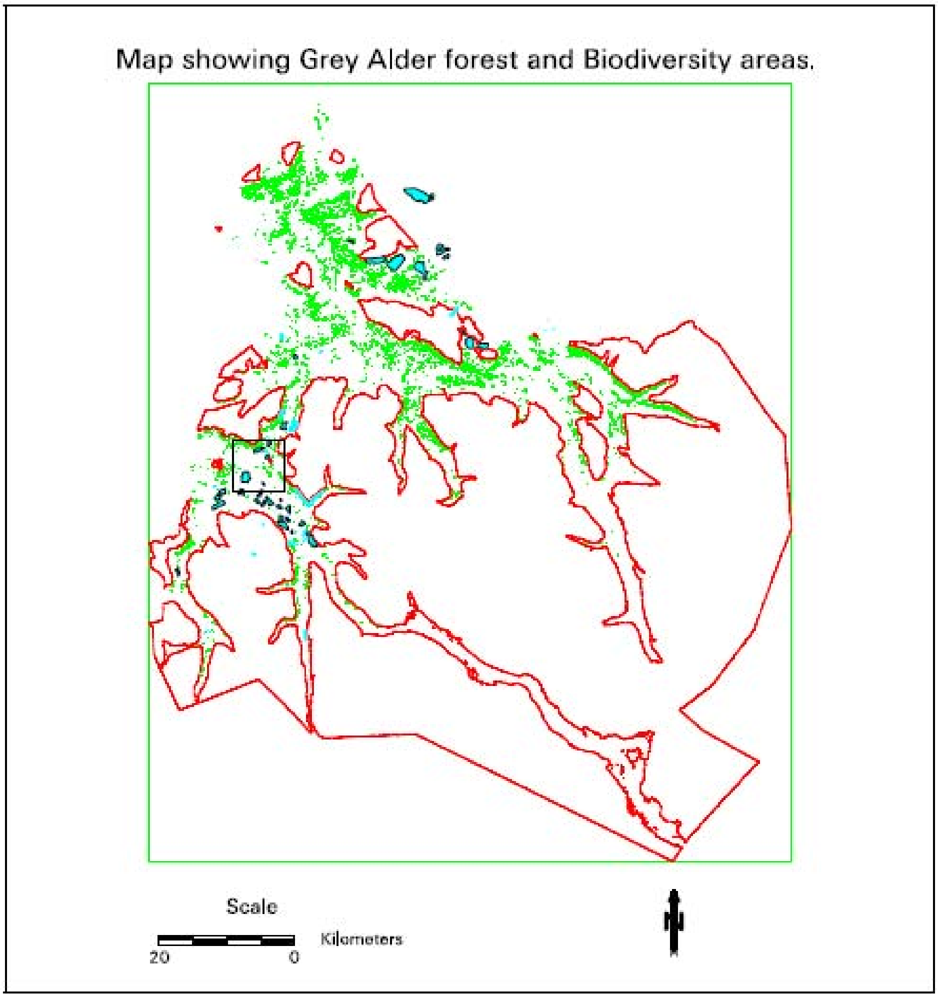

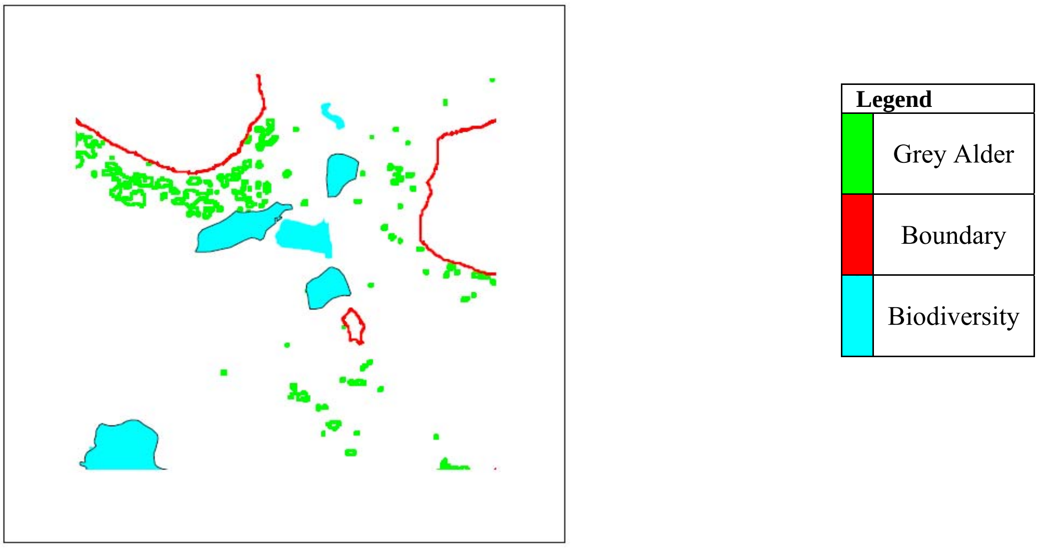

Figure 13. Showing the results of the <u>supervised July classification</u> of Landsat ETM+, with Grey Alder - Bird Cherry forest in green. Area totals 66 km^2. The smaller image is a close up of the larger image.

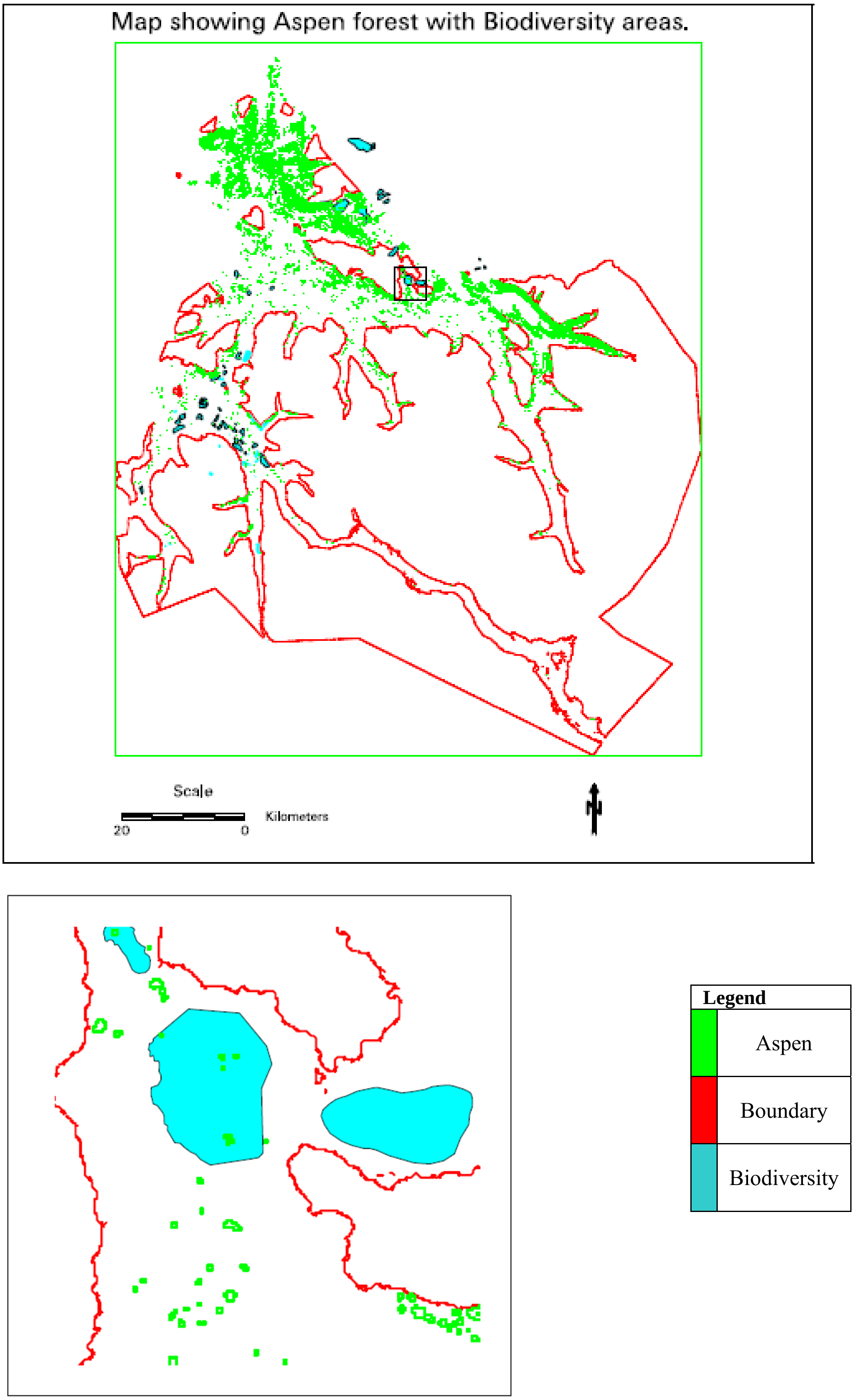

Figure 14. Map showing the results of the supervised July classification of Landsat ETM+, with Aspen forest in green. Area totals 97 km^2. The smaller image is a close up of the larger image.

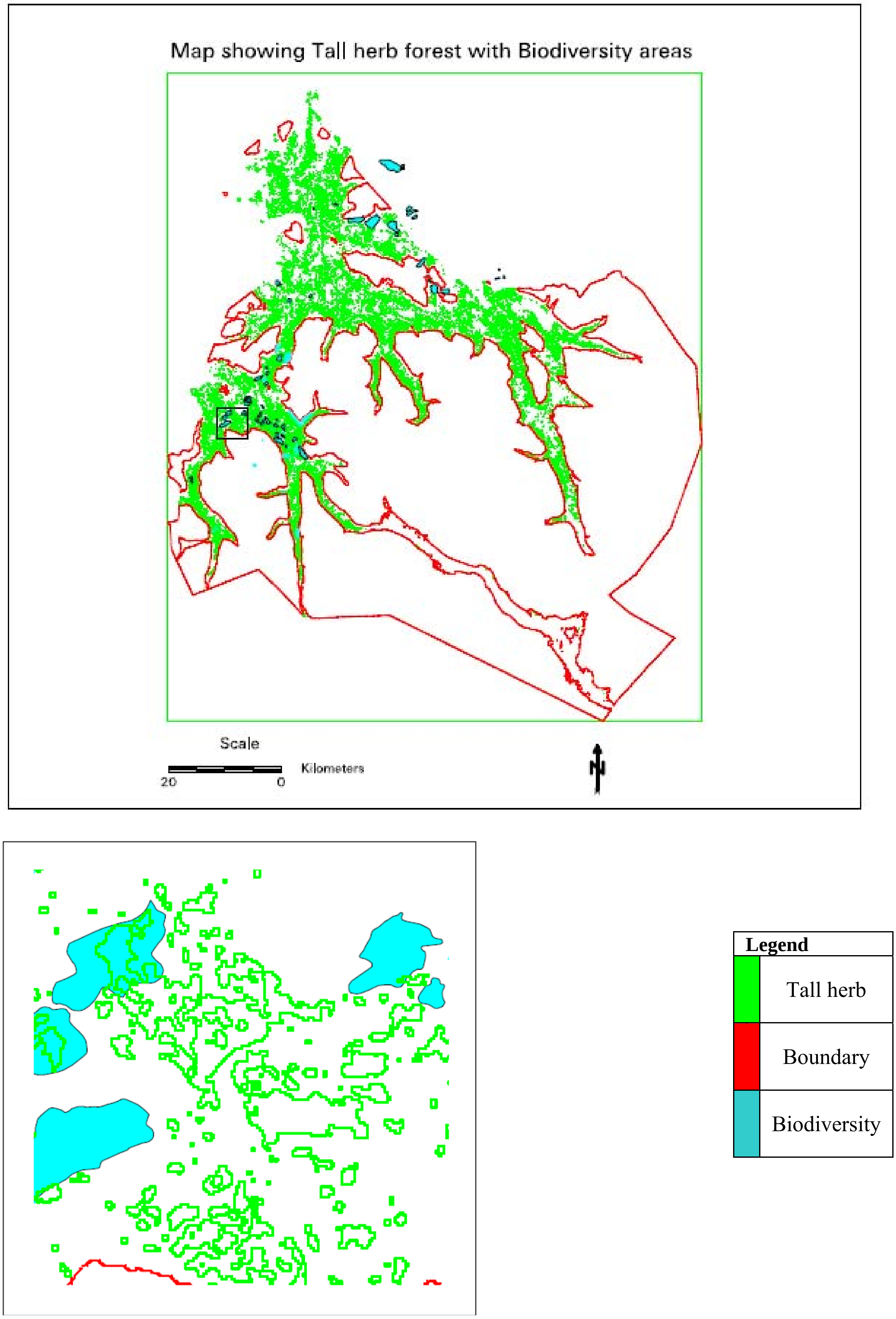

Figure 15. Map showing the results of the supervised July classification of Landsat ETM+, with Tall herb, Downy Birch forest in green. Area totals 268 km^2. The smaller image is a close up of the larger image.

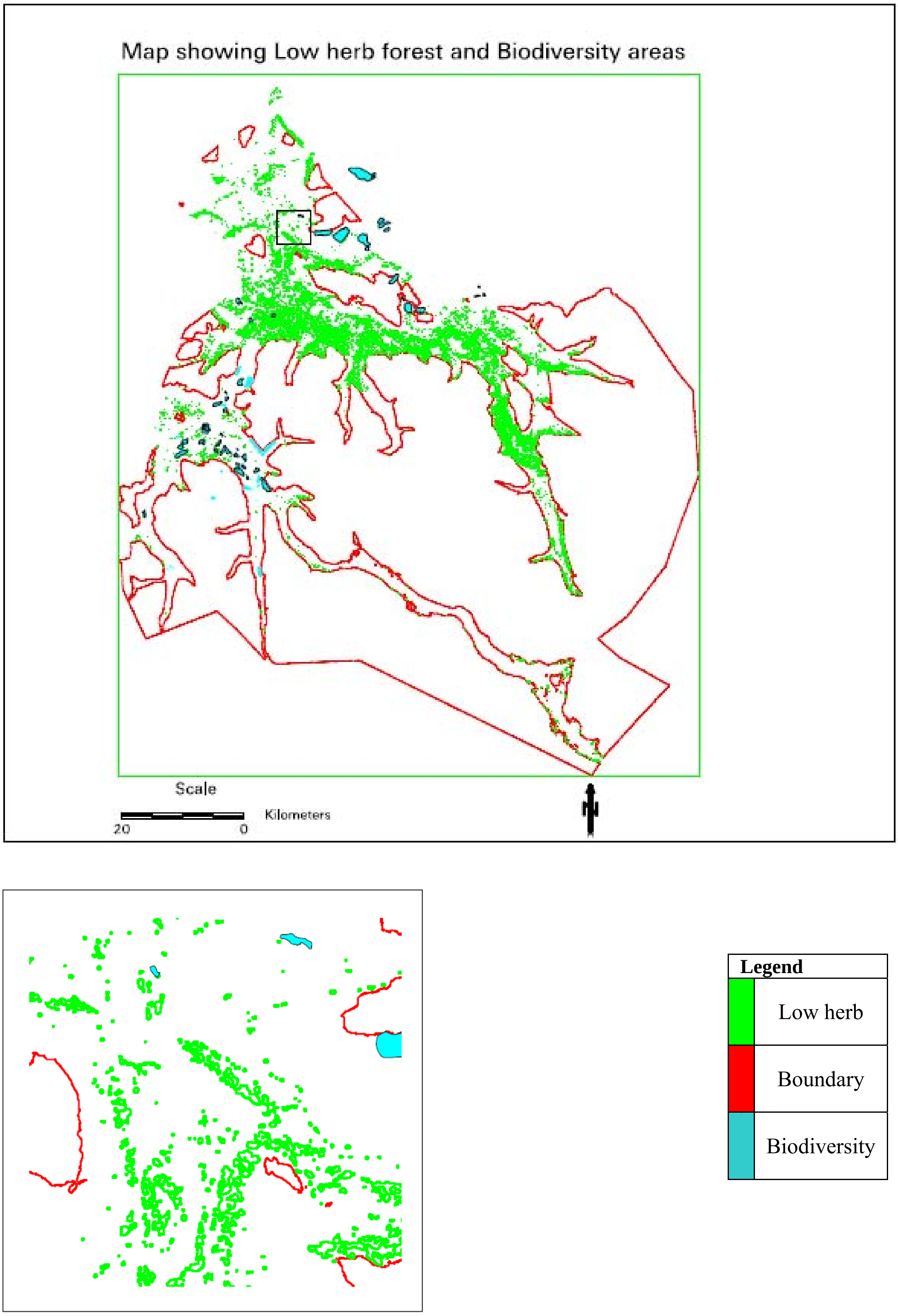

Figure 16. Map showing the results of the unsupervised July classification of Landsat ETM+, with Low herb, Downy Birch forest - with scattered tall herbs in green. Area totals 129 km^2. The smaller image is a close up of the larger image.

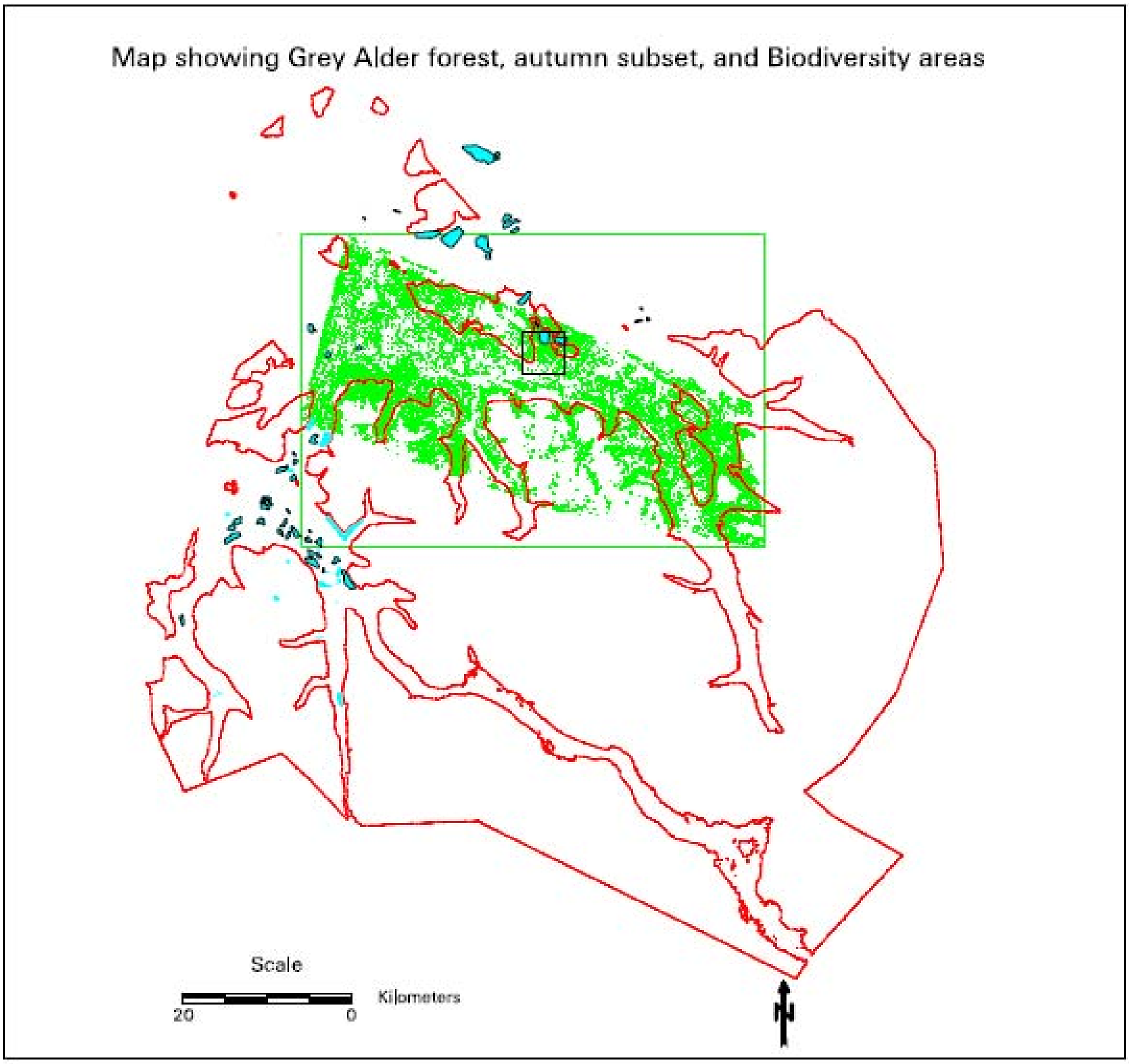

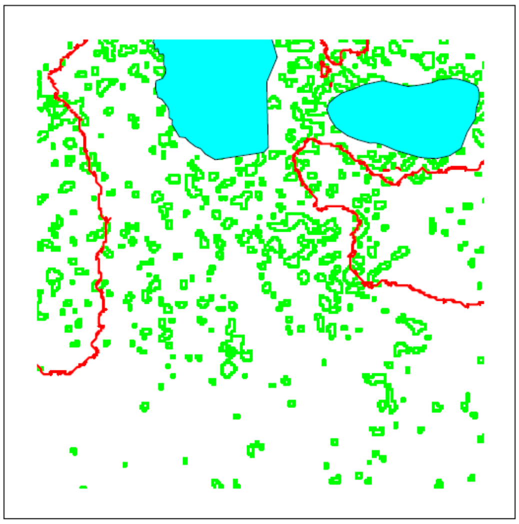

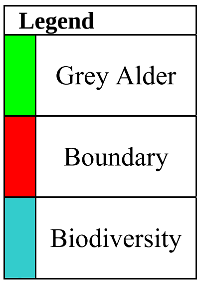

Figure 17. Map showing the results of the unsupervised September classification of Landsat ETM+, with GreyAlder - Bird Cherry forest in green. Area totals 149 km^2. The smaller image is a close up of the larger image.

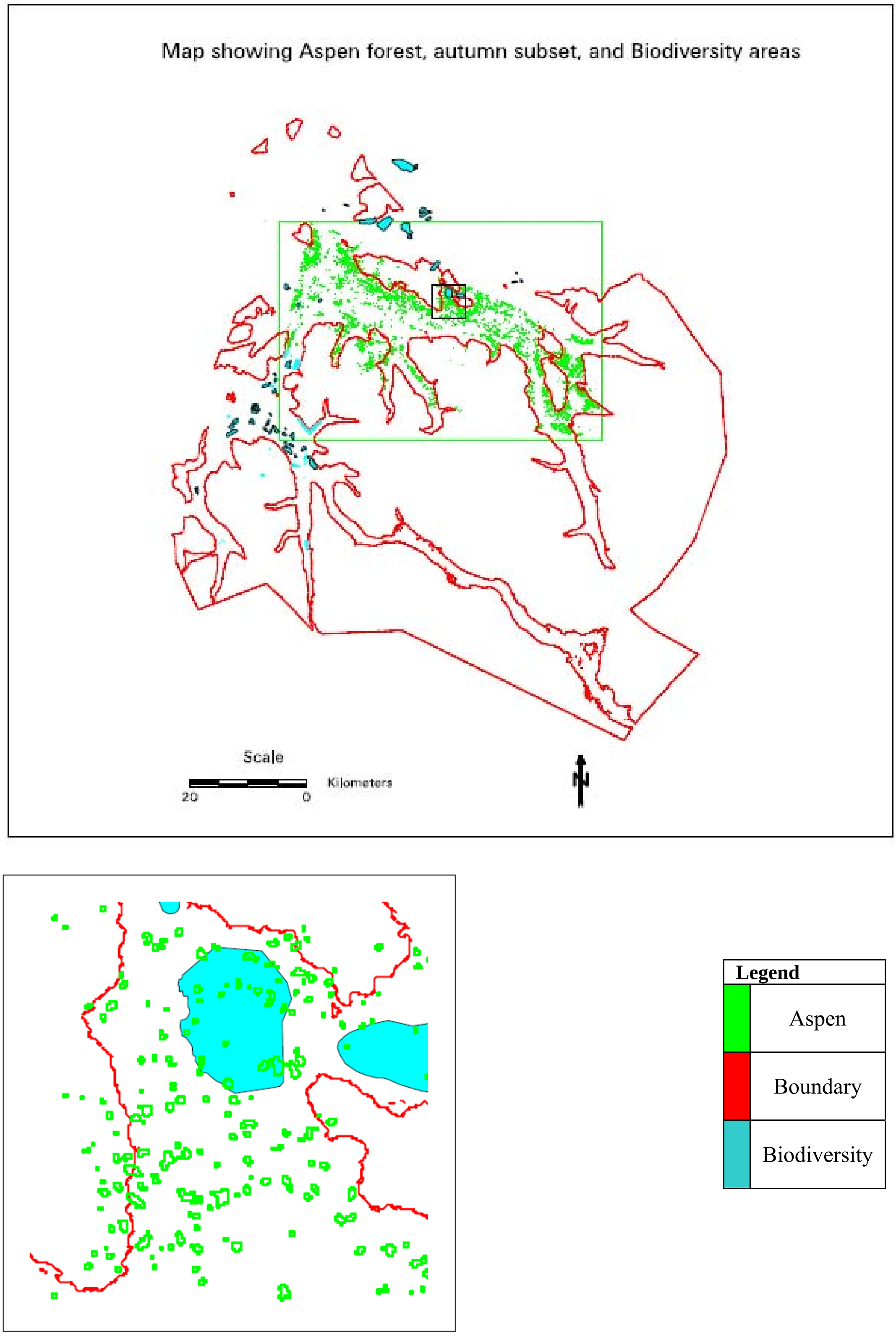

Figure 18. Map showing the results of the <u>unsupervised September classification</u> of Landsat ETM+, with Aspen forest in green. Area totals 39 km^2. The smaller image is a close up of the larger image.

5.4 NDVI data in combination with the vegetation maps

As explained in section 4.6 Vegetation indices, an NDVI was made of the study area and then it was modified to show only areas with values above 0.6. Afterward it was put in a model with the unsupervised July classification, rendering an image displaying only the richer parts of the four classes of broadleaved forests. This was then vectorized (in red) and put on an image showing the original four-class image (in shades of green). The Biodiversity map polygons (in turquoise) were then put on top and the results are shown in Figure 19 - 23. Figure 20 - 23 are close ups of the black squares in Figure 19. The unsupervised July classification was selected for this purpose, since it has the best overall accuracy; 60.59 %. No new accuracy assessment has been made on this composite.

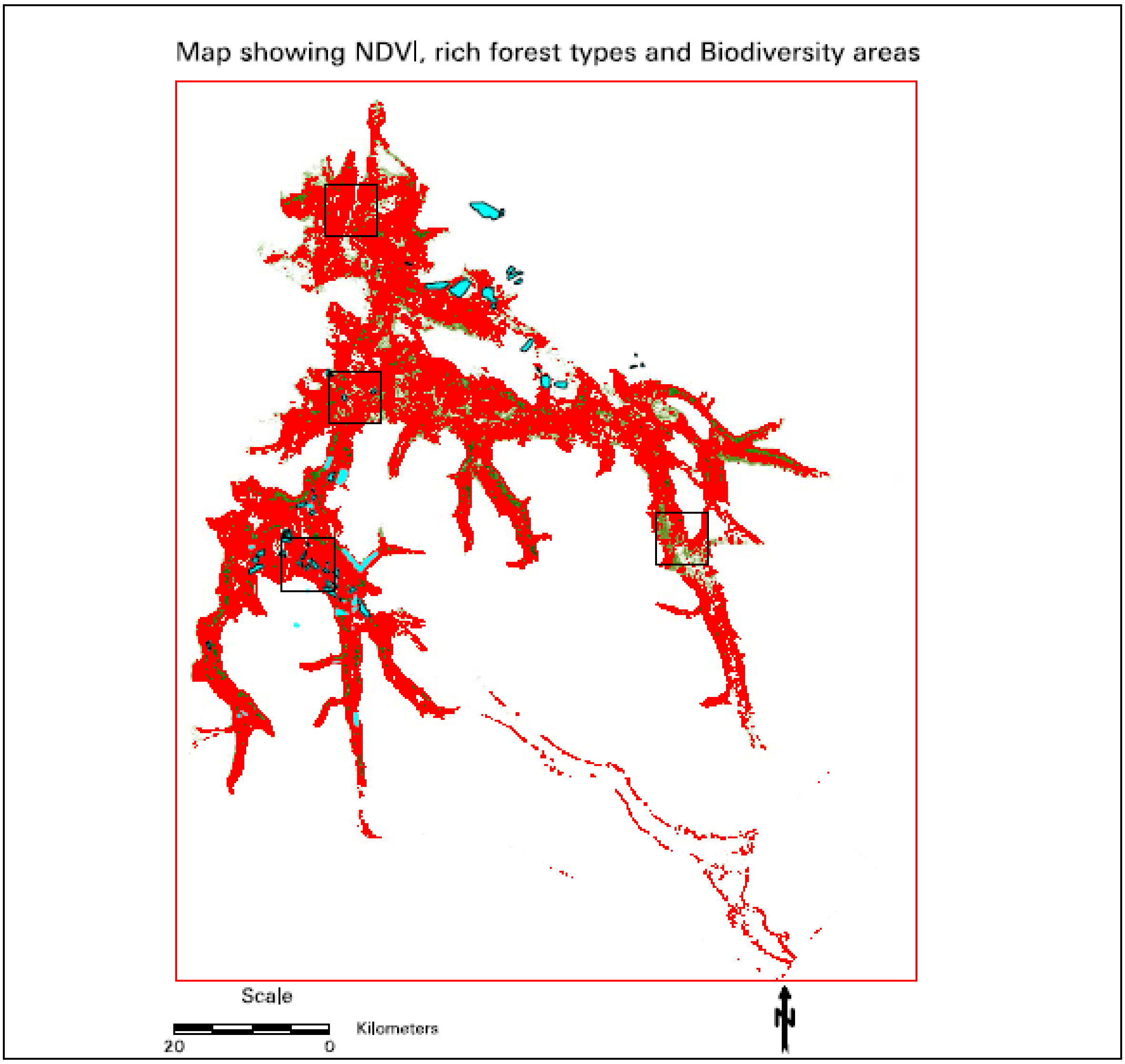

Figure 19. Map composite with thresholded NDVI.

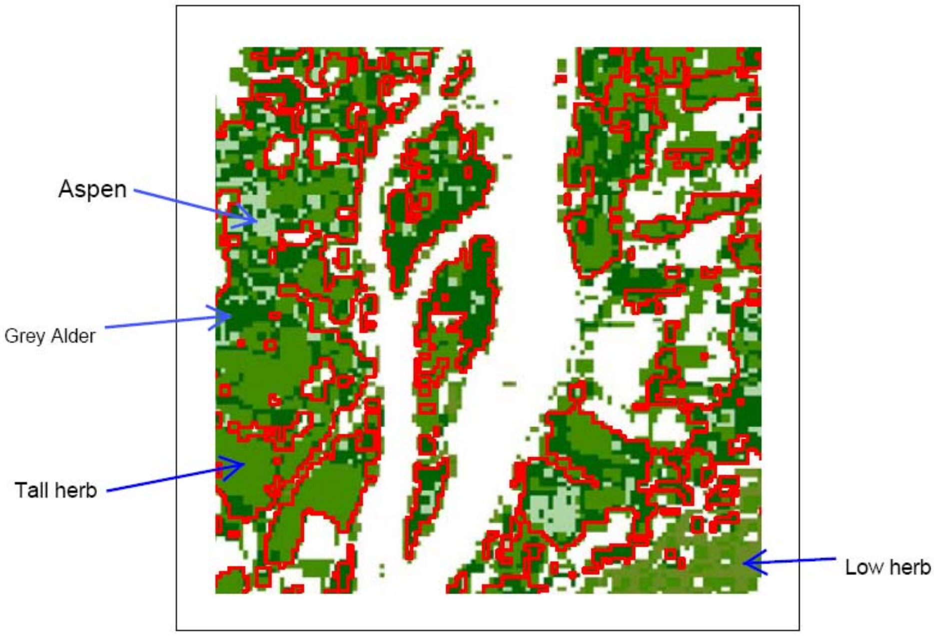

Figure 20. Close up of the upper left square in Figure 18.

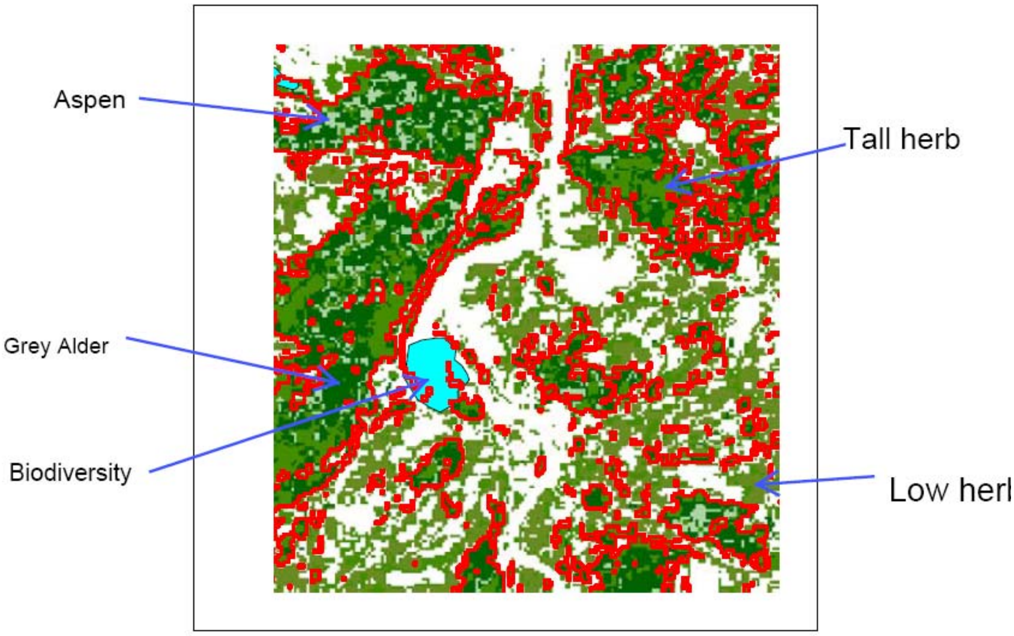

Figure 21. Close up of the middle left square in Figure 18.

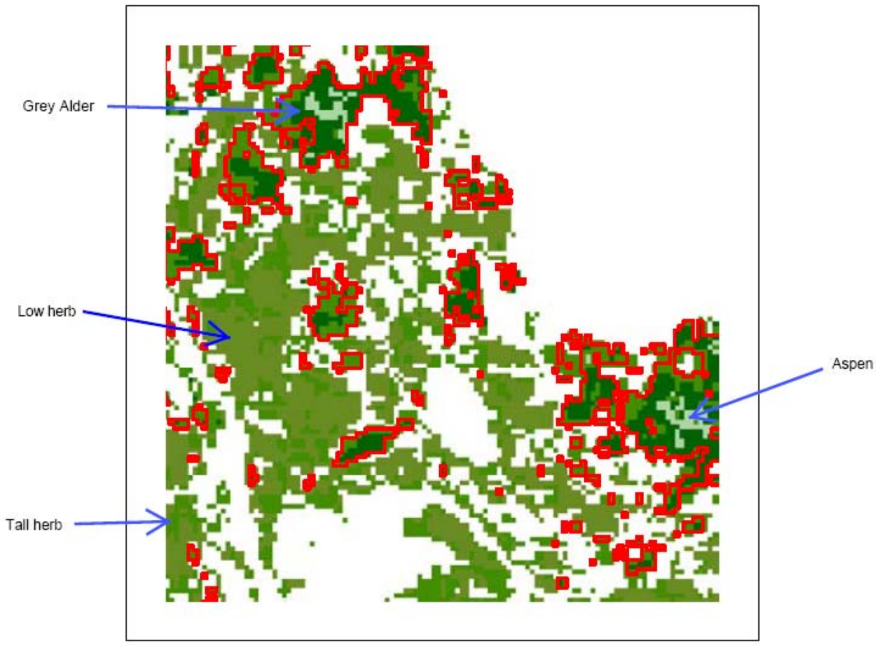

Figure 22. Close up of the right square in Figure 18.

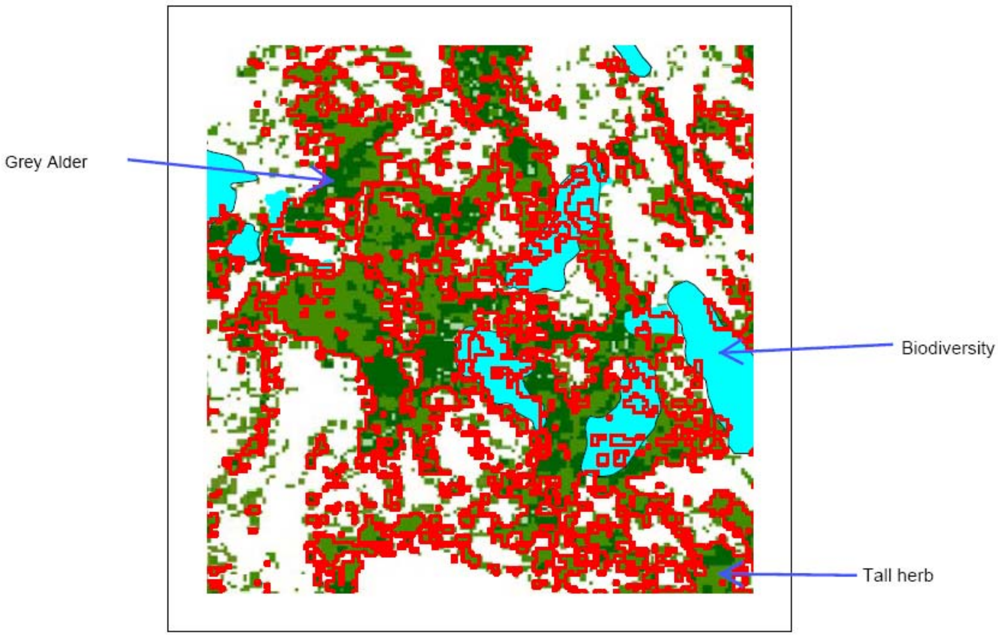

Figure 23. Close up of the lower left square in Figure 18.

6 Discussions

Results from this project, indicate that it is possible, to a certain degree, to map rich broadleaved forests using supervised and unsupervised per-pixel classification on Landsat ETM+ images, with an NDVI as ancillary data. The accuracy results implies that it is a bit difficult to differentiate between the four classes of rich broadleaved forest types in the study, but that the maps accuracy is sufficient to suggest areas that should undergo further mapping with regard to biodiversity. Especially when these maps are used with the inclusion of NDVI extracted maps.

6.1 Accuracy assessment

The overall accuracies in the three different classifications in this study are moderate to poor. A limited number of GCP may have influenced the classifications. Altogether 250 plots were collected, and divided in two groups, one for classification and one for accuracy assessment. As a supplement to these plots, a vegetation map was applied to extract about 150 points for use in the accuracy assessment of the non-rich broadleaved land cover types. The vegetation map produced by NIJOS in the beginning of the nineties can have errors. The accuracy assessment was limited by a small number of ground truth data for most of the land cover types. Of the rich broadleaves, only Grey Alder had more than 50 samples for use in the assessment. This renders the accuracy assessment less reliable. By Congalton's standard of accuracy (Congalton and Green, 1999), the assessments of the classifications here should only be considered tentative, and lead to a conservative interpretation of the images. This is especially true for the September image. Another problem that occurred during the image processing was that the imagery was partly influenced by two stripes; one stripe from the mosaicing of the two images constituting the study area and one broad stripe inherent in the image, probably as a consequence of some defect in the satellite. These two stripes might mean that there are spectral differences in the image and these irregularities may influence the classifications and indices produced in this thesis that could have led to misclassifications and lowered accuracy. The fact that Landsat 7 ETM+ lost its scan line corrector in 2003 leading to gaps in the registration of data might have also been a problem leading to mis-registrations of data before this corrector was completely damaged (USGS, 2006).

Despite the fact that the study area is below 500 meters above sea level, the terrain is steep in large parts of the two municipalities, being as they are, dominated by high mountains and cutting river valleys. A problem with per-pixel based forest stand mapping of Landsat ETM+ images, is that the spatial resolution is fairly low; both land cover and topography determine the spectral values in the images (Dorren et al., 2003). This condition will probably affect the classifications, at least in the narrower valleys and in the hillsides. Shadow effects, caused by topography, are facts that complicate the classification. This was especially apparent in the autumn image where there was major shadowing caused by a low sun, shaded by mountains.

6.2 To what extent can remote sensing data be used in forest type mapping?

At the local scale, I was unable to detect plant community types at hierarchical phyto-sociological levels as fine as I had hoped for at the outset of the project. For instance at the outset of the classifications, it was my intention to try to classify swamp forests, but this proved to be somewhat difficult. Reasons for this are, among other things, the insufficient GCP, the sampling scheme and that the fact that swamp forests show high spectral similarity to Grey Alder forests (Figure 6 and Figure 9). The difficulties could also be partly due to the medium pixel size of Landsat ETM+ also experienced by (Larsen, 2004) or due to classification method. After the first attempts of classification, swamp woodland was merged with Grey Alder forests. Larsen (2004) was able to map swamp forests with satisfactory results but he used high resolution data (1 and 6 meters spatial resolution) from the IKONOS-2 satellite as well as more sophisticated classification methods (sub-pixel classification). Kalliola and Syrjanen (Kalliola et al., 1991) concluded that satellite data often fail to distinguish many of the vegetation types recognized by the Finnish phyto-sociological school, though the major physiognomic categories are for the most part discernible. Most studies showing high classification accuracy do not follow such phyto-sociological schools like we and the Finnish researchers do, and get higher classification (more than 80 % overall classification accuracy) like Lobo & Gullison (Lobo and Gullison). Another finding is that Tall herb forest to a large extent has been misclassified as Grey Alder forest or Unclassified (mostly Lichen/bryophyte). Looking at Figure 7, we see that Tall herb forests have quite similar signatures to Grey Alder and indeed Aspen forests. Aspen seems to be better classified, although it might be mixed up with Grey Alder forest in particular. Unfortunately, there where only 19 samples in this class, which leads to uncertainties in the Accuracy Totals for the class. Low herb forest has a medium accuracy in the unsupervised July classification. But a very low number of samples for accuracy assessment render the Accuracy Totals of this class very uncertain.

According to Fremstad (Fremstad, 1997) there are floristical similarities between Tall herb, Downy Birch forest and Grey Alder – Bird Cherry forests on the one hand, and between these two and more Low herb characterized Downy Birch woodland on the other. Species content in each forest type will also vary with exposition and an eventual grazing pressure. Transitions like these are a problem in identifying swamp forests as well. There are often smooth transitions between bog-vegetation, swamp-vegetation and firm ground-vegetation. But from a management point of view, it is of lesser importance to classify a forest type as swamp forests or bog forests or something else according to phyto-sociological criteria, than to conserve the whole spectre of vegetation types for the future (Fremstad and Moen, 2001).

A typical forest in inland Troms is a mosaic of woodland types and different habitats. Grey Alder forests are quite often narrow and situated on floodplains, along meanders or in small river valleys. Aspen typically grows in-between other trees or in small groves. And in and around them are birch and pine forests with varied under-storey vegetation. There will almost always be an ever-changing gradient of different forests that are difficult to map because of their heterogeneity and small patch size. Land cover classification accuracy is affected by land cover heterogeneity and patch size, with the chances of a correct classification increasing with increasing patch size and decreasing heterogeneity (Smith et al., 2003). The low accuracy in the classifications can partly be explained by these factors. Landsat ETM+ remote sensing data is probably not the best suited imagery for mapping rich broadleaved woodland in this area. Studies have shown that a higher resolution might be better for mapping riparian vegetation (Muller, 1997), and this may also apply for other small woodland patches like Aspen groves. In his thesis Larsen (Larsen, 2004) suggests a six meter resolution for mapping subtypes of middle boreal rich alluvial forests. In addition, the accuracy of the gps coordinates may also be a source of error. In the best instances the accuracy was 5-7 meters, in the worst cases it was only 18-20 meters.

The rich broadleaved classes may have been somewhat overestimated, especially since there has been no effort made to exclude mixed classes. Another reason is that, when in doubt of a class, I have assigned it to a rich broadleaved class, preferably Grey Alder or Aspen. This has been done since these classes where the prime targets of this classification project. Nevertheless it may be better, to overestimate and to have too many sites to check in the field than to miss valuable habitats. Later, more ground truth data can be collected to verify or reject the classifications. The total forested area, according to these classifications, is 1472 km^2 for the supervised classification and 1319 km^2 for the unsupervised classification. According to Area statistics for 2006 by the Norwegian Mapping Authority (STATKART, 2006) forest constitutes approximately 1646 km^2 in the two municipalities. The two estimates are not too far from each other, nor from the official number. Still, forested areas have been somewhat underestimated in both classifications. The differences may be, among other things, due to a response to different classification systems, faulty classification on my part and the fact that my image is cut at 500 meters above sea level.

We may in the future be able to push the resolution of the forests types to increased detail using high resolution data such as SPOT 5, Quickbird, IKONOS or digital aerial photographs or images from different phenological stages, enabling biological diversity mapping at the local scale. Even the coarser regional scale of resolution (e.g.: Landsat) is sufficient (Wang et al., 2001), and my results concerning overall accuracy for the most important forest types like Grey Alder and Aspen forests showed satisfactory results (65.5 % and 57.1 %) as a baseline for sorting out areas with high chance for increased biological diversity.

6.3 Using vegetation maps in combination with NDVI

The NDVI composite in Figure 19, exemplifies how a classification can look when it is thresholded with an NDVI. It is important to notice that this image only conveys areas where the four forest types Grey Alder forest, Aspen forest, Tall herb forest and Low herb forest, have an NDVI above 0.6, according to one particular classification (the unsupervised classification of the July image). It does not imply that the classification has managed to classify all the richer areas as a rich broadleaved forest type. This image, in its present form, can be used to remove the areas that are not very rich in the broadleaved forest types. This would probably mask out some of the poorer areas that have been misclassified as a rich broadleaved forest type, when it is indeed a Lichen/bryophyte forest type. With the agricultural lands this will not work, since NDVI correlates directly with vegetation productivity (Pettorelli et al., 2005). A rich and productive green field has very high NDVI (Xiao et al., 2000/2001). In this instance an agricultural land cover map or land use map, can be used to mask out such areas.

Still there are the misclassifications among the rich broadleaved forest types themselves. Even though the accuracy is somewhat low, the classifications provide a good basis and a guide for further mapping. To some extent they imply what kind of rich broadleaved woodland we might expect to find in the area, and, more importantly, they provide us with a general idea of where to find any rich broadleaved forest type. Especially when the vegetation maps are used in combination with NDVI extracted data.

6.4 Concluding remarks: Vegetation maps as baseline maps for mapping of biological diversity

There is general consensus among natural heritage and conservation experts in Norway that the number of protected areas in most parts of the country must increase if biodiversity and ecosystem integrity are to be maintained in the long term. The previous biodiversity maps for the municipalities of Bardu and Målselv did not use baseline maps as forest maps or vegetation maps in order to stratify the mapping of hot spot or important areas for biodiversity. Only a part of Bardu municipality was mapped and within this area the mapping of areas with high level of biodiversity was easier to conduct (Strann et al., 2005), (Karl-Birger Strann, pers. com. 2007, Hans Tømmervik, pers. com. 2007).

Maps like the ones I have made in this study, can be used as starting points for mapping of the complete biodiversity in forests within these two municipalities. The scope of satellite imagery and the flexibility of GIS–generated visual tools (the base maps) can be manipulated manually for use in goal setting, management, and monitoring and they can also be used to generate digitized layers of information (Wang et al., 2001). The set of vegetation maps presented in Figures 12-17 reveal how patches and areas of main vegetation cover types are spread across the landscape. The vegetation types that are included in my survey may reflect the full complement of species and vegetation types that are found in forests throughout the two municipalities, even though the exact location of the different forest types and the border between them may be a little uncertain. A similar study was conducted in the Chigago Wilderness (Wang et al., 2001) and they found that information critical to the success of conservation efforts in the region includes a current vegetation map of the study, that are in a sufficient detail to allow quantitative goal setting for the region's biodiversity recovery plan. Also studies by (Lobo and Gullison) and (Gerard et al., 1998) showed that use of remote sensing is essential in mapping of biological diversity. Such maps also provide banks of geographically referenced data that make quantitative tracking of threats to areas with high biodiversity possible (Wang et al., 2001).

My study shows that there likely are several areas with high biodiversity, which have not yet been mapped in the area. According to my results, and based on the knowledge on how biodiversity has been mapped in Målselv and Bardu (Strann et al., 2005; Strann et al., 2005), I propose a further and more thorough study of the two municipalities.

7 Acknowledgements

This study was funded by the University of Tromsø, the Norwegian Institute for Nature Research and grants from the KOMETEN fund. Thank you for the support.

Many thanks to my supervisors Hans Tømmervik and Lennart Nilsen for their guidance and support in this project. I greatly appreciate that the Norwegian Institute for Nature Research, and all the friendly people working there, would have me roaming their corridors and writing my thesis with them. I would also like to thank Jarle W. Bjerke for his patient ability to answer my questions, and the guys next door; Knut and Bård for helping out with non-cooperative software, helpful advice and miscellaneous tasks. And, of course, a big thanks to my brother Jens Peter Nilssen and his sweetheart Hanne Stock Sunde (The Wielder of the Punctuation-whip) for helping out with the English language.

My fellow students and my friends here in Tromsø deserve a big thank you for being around. And, finally, the support of my mother, both financially and otherwise, has been invaluable.

8 References

Acres (2007) Geoscience Australia: Landsat Satellites. *In*,

Anderberg, Arne, Anderberg, Anna-Lena (2007) Den virtuella Floran. *In* N riksmuseet, ed. Naturhistoriska riksmuseet

Clarke KC (2003) Getting started with Geographic Information Systems. Prentice Hall

Congalton RG (2004) Putting the Map Back in Map Accuracy Assessment. Crc Press

Congalton RG, Green K (1999) Assessing the Accuracy of Remotely Sensed Data: Principles and Practices. Lewis Publishers

Delbart, N., Kergoat, L., Toan L, T., Lhermitte, J., Picard G (2005) Determination of phenological dates in boreal regions using normalized difference water index. Remote Sensing of Environment **97:** 26-38

Dorren, A. LK, Maier, B., Seijmonsbergen AC (2003) Improved Landsat-based forest mapping in steep mountainous terrain using object-based classification. Forest Ecology and Management **183:** 31-46

Fremstad E (1997) Vegetasjonstyper i Norge. Norsk Institutt for Naturforskning, Trondheim

Fremstad E, Moen A (2001) Truete vegetasjonstyper i Norge, Vol 2001-4. NTNU, Trondheim

Gao BC (1996) NDWI - A normalized difference water index for remote sensing of vegetation liquid water from space. Remote Sensing of Environment **58:** 257-266

Gerard, F., Wyatt, B., Millington, A., Wellens J (1998) The role of data from intensive sample plots in the development of a new method for mapping tropical forest tyepes using satellite imagery. *In* Dahlmeier, F Comiskey, J.A, eds, Forest biodiversity research, monitoring and modelling: Conceptual background and old world case studies. Man and the Biopshere (MAB) UNESCO and Parthenon Publishing Group, Paris and New York

Heywood I, Cornelius S, Carver S (2002) An Introduction to Geographical Information Systems. Pearsons. Prentice Hall

Jackson, D R, Pinter PJ (1986) Spectral response of architecturally different wheat canopies. Remote Sensing of Environment **20:** 43-56

Janssen, F. LL, Vanderwel FJM (1994) Accuracy Assessment of Satellite-Derived Land-Cover Data - a Review. Photogrammetric Engineering and Remote Sensing **60:** 419-426

Jensen JR (2005) Introductory Digital Image Processing. A Remote Sensing Perspective. Pearson Education Inc

Johnston CA (1998) Geographic Information Systems in Ecology. Blacwell Science

Justice CO, Townshend JRG, Holben BN, Tucker CJ (1985) Analysis of the phenology of global vegetation using meteorological satellite data. International Journal of Remote Sensing **6:** 1271-1318

Kalliola, R., Syrjanen K (1991) To what extent are vegetation types visible in satellite imagery. Ann. Bot. Fennici **28:** 45-57.

Larsen BW (2004) Spatial challenges in satellite based vegetation mapping; Integration of satellite data in a Geographic Information System for detection and fine-scale mapping of rich alluvial forests in Målselv and Bardu, northern Norway. Master Project. University of Tromsø

Leica Geosystems (2006) Erdas Imagine 9.1. *In*,

Lid, J., Lid DT (2005) Norsk Flora, Vol Det Norske Samlaget, Oslo

Lillesand, M. T, Kiefer RW (2000) Remote sensing and image interpretation. John Wiley & Sons, Inc.

Lobo A, Gullison RE (1998) Mapping the tropical landscapes of Beni (Bolivia) from Landsat-TM imagery: Beyond the "Forest/NON Forest Legend. *In* Dahlmeier, F, JA Comiskey, eds, Forest biodiversity research, monitoring and modelling: Conceptual background and old world case studies. Man and the Biopshere (MAB) Vol 20. UNESCO and Parthenon Publishing Group. , Paris and New York, pp 159-182
Moen A (1998) Nasjonalatlas for Norge: Vegetasjon. Statens Kartverk, Hønefoss
Muller E (1997) Mapping riparian vegetation along rivers: old concepts and new methods. Aquatic Botany **58:** 411-437
Myers, W., Patil, G.P., Taillie C (1999) Cluster co-ordinated composites of diverse datasets on several spatial scales for designing extensive environmental sample surveys: prospectus on promising protocols. *In* S Ghosh, ed, Multivariate Analysis, Design of Experiments, and Survey Sampling. Marcel Dekker Incorporation. , New York, pp 119-133
Myers, W., Shelton R (1998) Survey methods for ecosystem management. Wiley-Interscience, New York.
Myneni, B. R, Asrar, G., Tanre, D., Choudhury BJ (1992) Remote-Sensing of Solar-Radiation Absorbed and Reflected by Vegetated Land Surfaces. Ieee Transactions on Geoscience and Remote Sensing **30:** 302-314
NASA (2007) Earth Observatory. *In* NASA, ed, Vol 2007. http://earthobservatory.nasa.gov/Library/MeasuringVegetation/measuring_vegetation_2.html
NASA (2007) The Landsat Program. *In*. http://landsat.gsfc.nasa.gov/about/landsat7.html
Naturforvaltning Df (1999) Kartlegging av naturtyper., Vol 13. DN
NGU (2007) Løsmasser. *In*. http://www.ngu.no/kart/losmasse/
NIJOS (1991) Vegetasjonskart over Bardu. *In*. The Norwegian Forest and Landscape Institute, p
Pettorelli, N., Vik, O. J, Mysterud, A., Gaillard, M. J, Tucker, J. C, Stenseth, C. N (2005) Using the satellite-derived NDVI to assess ecological responses to environmental change. Trends in Ecology & Evolution **20:** 503-510
Prince SD (1991) Satellite remote sensing of primary production - Comparison of results for Sahelian grasslands 1981-1988. International Journal of remote sensing **12:** 1301-1311
Rees WG (1990) Physical Principles of Remote Sensing. Cambridge University Press, Cambridge
Reichert, G.C., Crown PH (1984) Identification of winter wheat using Landsat MSS data. Canadian Journal of Remote Sensing **10:** 111-120
Santos, R., Ohashi, T., Yoshida, T., Ejima TT (1998) Filtering and segmentation of digitized land use map images. . International Journal on Document Analysis and Recognition **1:** 167-174
Sellers PJ (1986) Canopy reflectance, photosynthesis and transpiration. International Journal of Remote Sensing **6:** 1335-1372
Slayback, A. D, Pinzon, E. J, Los, O. S, Tucker CJ (2003) Northern hemisphere photosynthetic trends 1982-99. Global Change Biology **9:** 1-15
Sluiter, R., Zeijlmans M (2002) Remote Sensing - A Tool for Environmental Observations. *In* d Jong, S.M., eds, Lecture notes. Remote Sensing 2. Utrecht University, Utrecht
Smith, H. J, Stehman, V. S, Wickham, D. J, Lang LM (2003) Effects of landscape characteristics on land-cover class accuracy. Remote Sensing of Environment **84:** 342-349
State of the Environment Norway (2006) State of the Environment Norway. *In* DN

STATKART (2006) Arealstatistikk for 2006. *In* Å Hadler, ed. Norwegian Mapping Authority

Strann, K, Tømmervik, H, Frivoll, V, Iversen, M, Johnsen T (2005) Biologisk Mangfold. Bardu Kommune. *In* Nina Rapport 58, Vol 58

Strann KB, Frivoll, V, Iversen, M, Johnsen, T, Jacobsen K-O (2005) Biologisk mangfold. Målselv kommune. *In* NINA Rapport 46,

Street, L., Street S (2001) The importance of Aspens for lichen. *In* The Biodiversity and Management of Aspen woodlands, Kingussie, Scotland

Systad, G.H, Tømmervik, H, Strann K-B (2000) Flora og fauna registrering i Målselvutløpet Naturreservat, samt revisjon av vegetasjonskart. *In* Oppdragsmelding,

Tucker, J. C, Sellers PJ (1986) Satellite remote sensing of primary production. International Journal of Remote Sensing **7:** 1395-1416

USGS (2006) Landsat Project, Project Description. *In*. U.S. Department of the Interior | U.S. Geological Survey

Van Genderen JL, Lock, B.F., Vass, P.A. (1978) Remote sensing: Statistical testing for thematic map accuracy. Remote Sensing of Environment **7(1):** 3-14

Wang, Y, Moskovits DK (2001) Tracking Fragmentation of Natural Communities and Changes in Land Cover: Applications of Landsat Data for Conservation in an Urban Landscape (Chicago Wilderness). Conservation Biology **15 (4): 835-843** 835-843

Werth S (2001) Key factors for epiphytic macrolichen vegetation in deciduous forests of Troms county, northern Norway: human impact, substrate, climate or spatial variation? Master thesis. University of Tromsø

Worrell R (1995) European Aspen (Populus-Tremula L) - a Review with Particular Reference to Scotland .1. Distribution, Ecology and Genetic-Variation. Forestry **68:** 93-105

Xiao X, Boles S, Frolking S, Salas W, Moore-III B, Li C, He L, Zhao R (2000/2001) Landscape-scale characterization of cropland in China using

Vegetation and Landsat TM images.

9 Appendices

Appendix 1 - List of species

Table 15. List of species recorded in the field. Englisn names according to (Anderberg et al., 2007) and Norwegian names according to (Lid et al., 2005).

Scientific name	**English name**	**Norwegian name**
Lycopodium annotinum	Interrupted Clubmoss	Stri kråkefot
Equisetum arvense	Field Horsetail	Åkersnelle
Equisetum pratense	Shady Horsetail	Engsnelle
Equisetum sylvaticum	Wood Horsetail	Skogsnelle
Equisetum palustre	Marsh Horsetail	Myrsnelle
Equisetum fluviatile	Water Horsetail	Elvesnelle
Matteuccia struthiopteris	Ostrich Fern	Strutseveng
Athyrium filix-femina	Lady-fern	Skogburkne
Gymnocarpium dryopteris	Oak Fern	Fugletelg
Dryopteris filix-mas	Male-fern	Ormetelg
Dryopteris dilatata	Broad Buckler-fern	Geittelg
Dryopteris expansa	Northern Buckler-fern	Sauetelg
Phegopteris connectilis	Beech Fern	Hengjeveng
Pinus sylvestris	Scots Pine	Vanleg furu
Picea abies	Norway Spruce	Gran
Juniperus communis	Common Juniper	Einer
Salix glauca ssp. glauca	Willow	Sølvvier
Salix lapponum	Downy Willow	Lappvier
Salix myrsinifolia ssp. myrsinifolia	Dark-leaved Willow	Vanleg svartvier
		Setervier
Salix phylicifolia	Tea-leaved Willow	Grønvier
Salix caprea	Goat Willow	Selje
Salix pentandra	Bay Willow	Istervier
Populus tremula	Aspen	Osp
Betula pubescens	Downy Birch	Bjørk
Betula nana	Dwarf Birch	Dvergbjørk
Alnus incana ssp. incana	Grey Alder	Vanleg gråor
Urtica dioica	Common Nettle	Stornesle
Rumex acetosa	Common Sorrel	Engsyre
Bistorta vivipara	Alpine Bistort	Harerug
Stellaria nemorum	Wood Stitchwort	Skogstjerneblom
Cerastium fontanum	Common Mouse-ear	Vanleg arve
Cerastium fontanum ssp. fontanum	Common Mouse-ear	Skogarve
Silene dioica	Red Campion	Raud jonsokblom
Caltha palustris	Marsh-marigold?	Bekkeblom
Trollius europaeus	Globeflower	Ballblom
Actaea spicata	Baneberry	Trollbær
Ranunculus auricomus	Goldilocks Buttercup	Nyresoleie
Ranunculus acris	Meadow Buttercup	Engsoleie
Ranunculus repens	Creeping Buttercup	Krypsoleie
Thalictrum alpinum		Fjellfrøstjerne

Cardamine pratensis ssp. dentata	Cuckooflower	Sumpkarse
Erysimum hieracifolium		Berggull
Saxifraga stellaris	Starry Saxifrage	Stjernesildre
Ribes spicatum	Downy Currant	Villrips
Filipendula ulmaria	Meadowsweet	Mjødurt
Geum rivale	Water Avens	Enghumleblom
Potentilla palustris	Marsh Cinquefoil	Myrhatt
Potentilla erecta	Tormentil	Tepperot
Rubus chamaemorus	Cloudberry	Molte
Rubus arcticus	Arctic Bramble	Åkebær
Rubus saxatilis	Stone Bramble	Tågebær
Rubus idaeus	Raspberry	Bringebær
Sorbus aucuparia ssp. aucuparia	Rowan	Vanleg rogn
Prunus padus ssp. padus	Bird Cherry	Vanleg hegg
Oxalis acetosella	Wood-sorrel	Gaukesyre
Geranium sylvaticum	Wood Crane's-bill	Skogstorkenebb
Viola biflora		Fjellfiol
Viola palustris	Marsh Violet	Myrfiol
Viola epipsila		Stor myrfiol
Viola riviniana	Common Dog-violet	Skogfiol
Chamerion angustifolium	Rosebay Willowherb	Geitrams
Chamaepericlymenum suecicum	Dwarf Cornel	Skrubbær
Anthriscus sylvestris	Cow-Parsley	Hundekjeks
Angelica sylvestris	Wild Angelica	Sløkje
Angelica archangelica	Garden Angelica	Kvann
Pyrola minor	Common Wintergreen	Perlevintergrøn
Orthilia secunda	Serrated Wintergreen	Nikkevintergrøn
Phyllodoce caerulea	Blue Heath	Blålyng
Calluna vulgaris	Heather	Røsslyng
Vaccinium vitis-idaea	Cowberry	Tytebær
Vaccinium uliginosum	Bog Bilberry	Blokkebær
Vaccinium myrtillus	Bilberry	Blåbær
Vaccinium oxycoccus ssp. microcarpum	Small Cranberry	Småtranebær
Empetrum nigrum	Crowberry	Krekling
Trientalis europaea	Chickweed Wintergreen	Skogstjerne
Galium palustre ssp. palustre	Common Marsh-bedstraw	Lita myrmaure
Myosotis decumbens		Fjellminneblom
Myosotis sylvatica	Wood Forget-me-not	Skogminneblom
Melampyrum pratense	Common Cow-wheat	Stormarimjelle
Melampyrum sylvaticum	Small Cow-wheat	Småmarimjelle
Bartsia alpina	Alpine Bartsia	Svarttopp
Pinguicula vulgaris	Common Butterwort	Tettegras
Linnaea borealis	Twinflower	Linnea
Valeriana sambucifolia	Common Valerian	Vendelrot
Solidago virgaurea	Goldenrod	Gullris
Omalotheca norvegica	Highland Cudweed	Setergråurt
Cirsium heterophyllum	Melancholy Thistle	Kvitbladtistel
Crepis paludosa	Marsh Hawk's-beard	Sumphaukeskjegg
Cicerbita alpina	Alpine Blue-sow-thistle	Turt
Taraxacum officinale	Dandelion	Løvetenner
Hieracium sylvatica		Skogsvæver
Paris quadrifolia	Herb-Paris	Firblad

Polygonatum verticillatum	Whorled Solomon's-seal	Kranskonvall
Dactylorhiza maculata	Heath Spotted-orchid	Flekkmarihand
Dactylorhiza fuchsii	Common Spotted-orchid	Skogmarihand
Coeloglossum viride	Frog Orchid	Grønkurle
Luzula pilosa	Hairy Wood-rush	Hårfrytle
Eriophorum vaginatum	Hare's-tail Cottongrass	Torvull
Eriophorum angustifolium	Common Cottongrass	Duskull
Carex chordorrhiza	String Sedge	Strengstorr
Carex nigra ssp. juncella	Common Sedge	Stolpestorr
Carex aquatilis ssp. aquatilis	Water Sedge	Nordlandsstorr
Carex vaginata	Sheathed Sedge	Slirestorr
Carex paupercula	Tall Bog-sedge	Frynsestorr
Carex rostrata	Bottle Sedge	Flaskestorr
Milium effusum	Wood Millet	Myskegras
Agrostis capillaris	Common Bent	Engkvein
Calamagrostis phragmitoides	Scandinavian Small-reed	Skogrøyrkvein
Deschampsia cespitosa ssp. cespitosa	Tufted Hair-grass	Sølvbunke
Avenella flexuosa	Wavy Hair-grass	Smyle
Melica nutans	Mountain Melick	Hengjeaks
Poa nemoralis	Wood Meadow-grass	Lundrapp
Elymus caninus	Bearded Couch	Hundekveke

Appendix 2 - Dendrogram

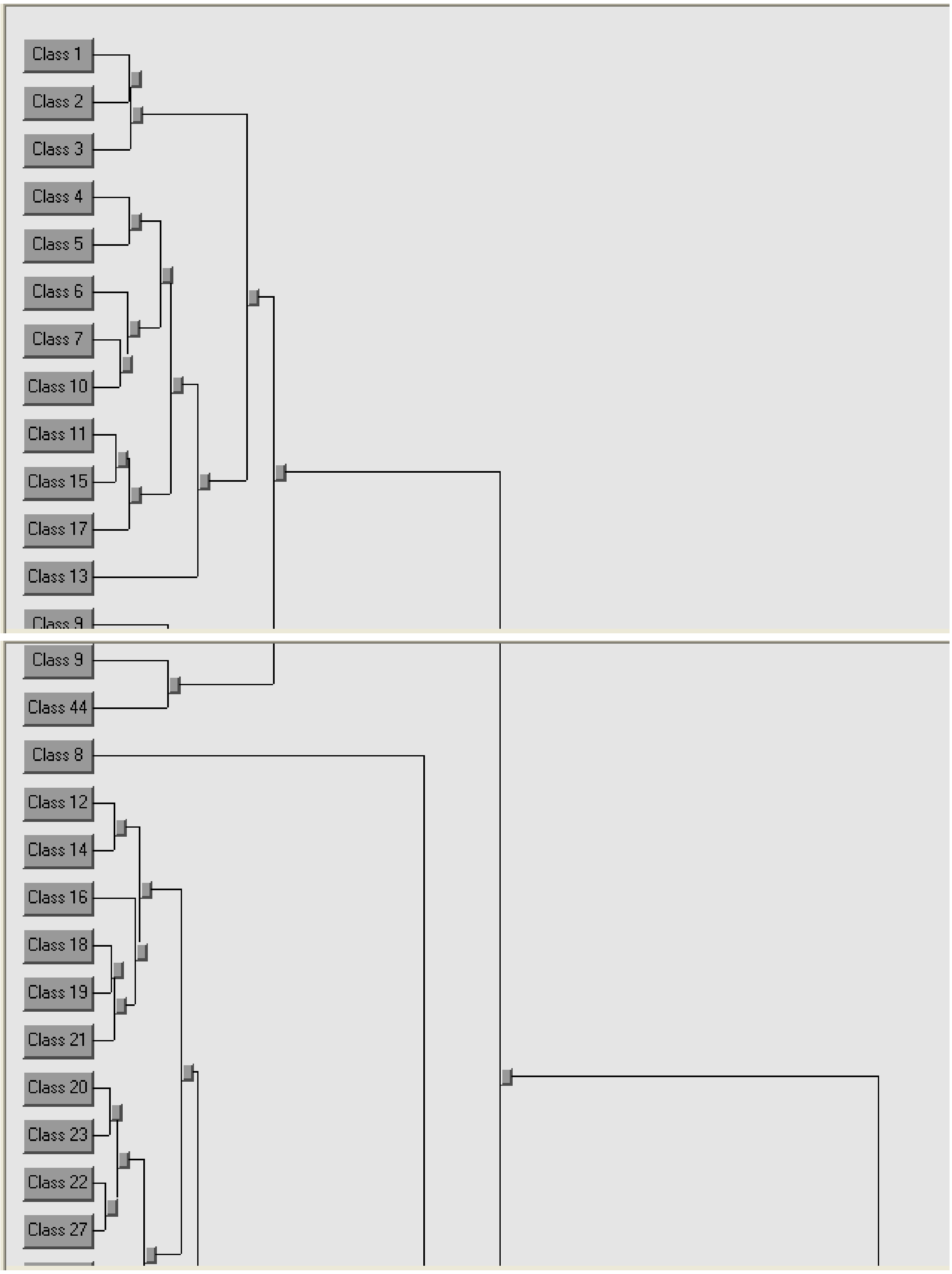

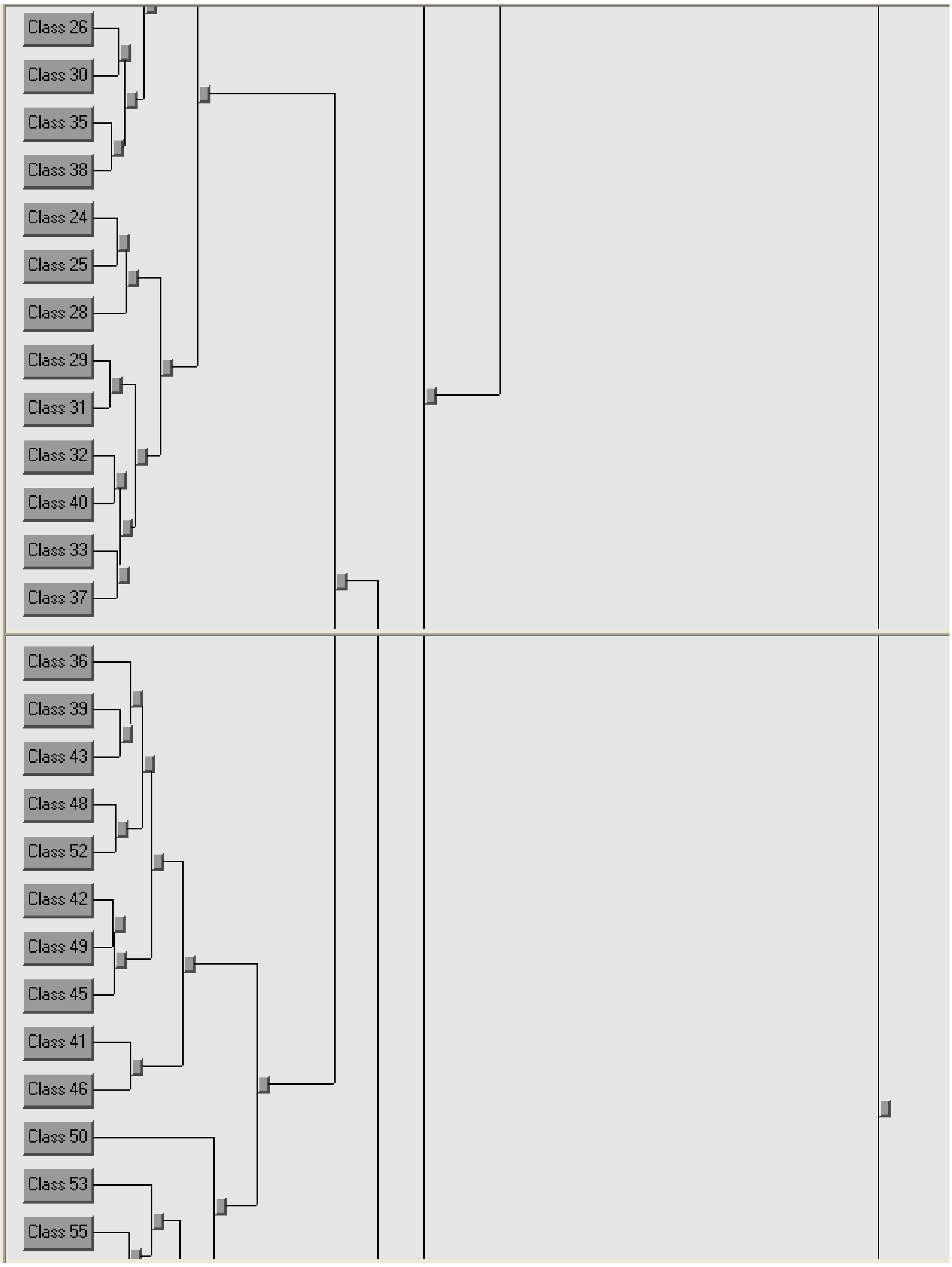
Class 26
Class 30
Class 35
Class 38
Class 24
Class 25
Class 28
Class 29
Class 31
Class 32
Class 40
Class 33
Class 37
Class 36
Class 39
Class 43
Class 48
Class 52
Class 42
Class 49
Class 45
Class 41
Class 46
Class 50
Class 53
Class 55

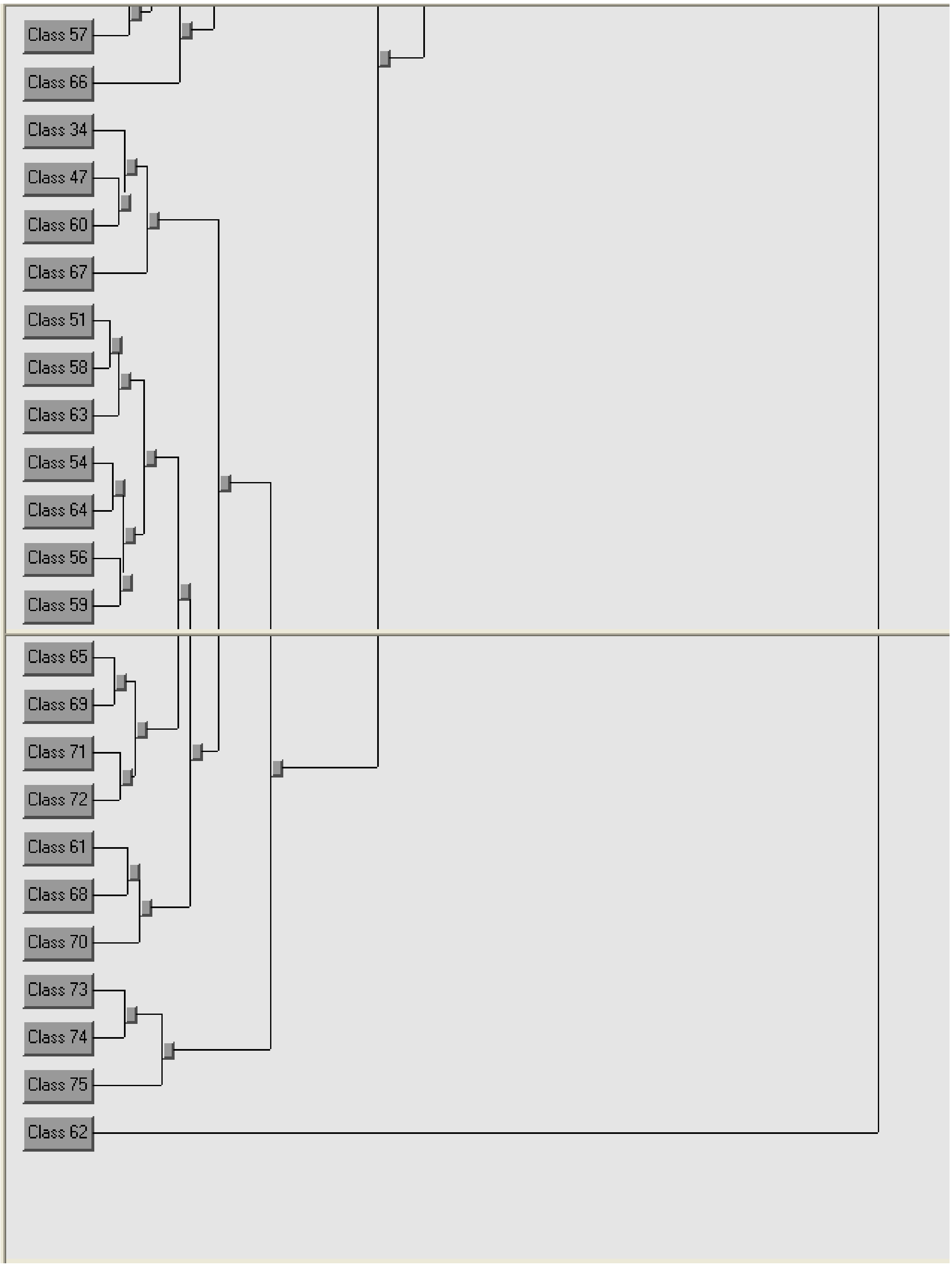

Figure 24. Dendrogram displaying how the 75 signatures from the unsupervised July classification are clustered.

Appendix 3 - List of classes

Description of classes: Descriptions are taken from Fremstad's"Vegetasjonstyper i Norge" (Vegetation types of Norway) (Fremstad, 1997). Descriptions are based on how these vegetation types appear in the study area.

1. Grey Alder – Bird Cherry forest (Abbreviated Grey Alder).

    Forest dominated by Grey Alder (*Alnus incana* ssp. *Incana*) alone or mixed with Downy Birch (*Betula pubescens* ssp.*pubescens*), Bird Cherry (*Prunus padus*), Goat Willow (*Salix caprea* ssp. *caprea*) and Dark-leaved Willow (*Salix myrsinifolia* coll). Tall and dense field layer dominated by herbs and high grasses, often with a characteristic spring aspect of geophytes. Field layer little to well developed, usually rich in species and in demanding species. Examples of plants found here are Downy Currant (*Ribes spicatum*), Meadowsweet (*Filipendula ulmaria*) and Ostrich Fern (*Matteuccia struthiopteris*).

    Found in sediments along rivers, in ravines and on screes, rock fall material in hillsides. This is a highly productive forest type.

    Corresponds to C3 and E in Fremstad.

2. Rich swamp woodland

    Highly developed tree layer of (in North Norway) Grey Alder (*Alnus incana*), Downy Birch (*Betula pubescens*) and Dark-leaved Willow (*Salix myrsinifolia*). The shrub layer is usually sparse or lacking, the field layer on the other hand is well developed with tall grasses and herbs. Found on wet and nutritious ground. Not a very common vegetation type. Typical plant found here are Cow-Parsley (*Anthriscus sylvestris*), Scandinavian Small-reed (*Calamagrostis canescens*), Water Avens (*Geum rivale*) and Marsh-marigold (*Caltha palustris*).

    Corresponds to E in Fremstad.

3. Aspen

    Aspen (*Populus tremula*) is not treated as a separate woodland type, but is mentioned as a major constituent in several other types:

    "From BN to NB blueberry forest exists with a tree layer of Aspen, especially in hillsides with a favourable exposition. Blueberry-aspen forests are poorly examined and are not counted as a class of their own at this time." and *"Low herb woodland with a strong element or dominance of Aspen is found in several regions (N-MB)"* Fremstad (my translation). Aspen is a wide ranging tree species(Worrell, 1995), in Europe it extends from 71° N in Norway and southwards to northern Africa and it extends far east to Japan, still aspen woodland is poorly examined especially in the north of Norway.

    Does not correspond to a class in Fremstad.

4. Tall herb, Downy Birch forest (Abbreviated Tall herb).

Nutritious forests dominated by ferns and/or herbs. Downy Birch or Grey Alder dominates the tree layer. This is usually a species rich vegetation type on moist/fresh and nutritious ground, often affected by percolating water.

Alpine Blue-sow-thistle (*Cicerbita alpina*) and Globeflower (*Trollius europaeus*) are examples of typical herbs. Also large grasses and ferns are represented e.g. Wood Millet (*Milium effusum*) and Oak Fern (*Gymnocarpium dryopteris*). This is a very productive forest type.

Corresponds to C1 and C2, except C2c, in Fremstad.

5. Low herb, Downy Birch forest, with scattered tall herbs (Abbreviated Low herb).

This is an intermediate between the Tall herb, Downy Birch forest and Low herb woodland. It is a drier version of the tall herb type. It is found on nutrition rich, well drained ground. Usually it has a mix of low herbs and grasses, and poorly developed, tall herbs. In addition to Downy Birch species like Wood Crane's-bill (*Geranium sylvaticum*), Stone Bramble (*Rubus saxatilis*), Goldenrod (*Solidago virgaurea*) and Small Cow-wheat (*Melampyrum sylvaticum*) are found in this vegetation type.

Corresponds to C2c in Fremstad.

6. Lichen/bryophyte and dwarf shrub woodland (Abbreviated Lichen/bryophyte).

This class contains several poorer woodland types consisting of Scots Pine (*Pinus sylvestris*) and Downy Birch. It is dominated by heather, lichens and moss in its field and ground layers. Crowberry (*Empetrum nigrum*), Cowberry (*Vaccinium vitis-idaea*), Interrupted Clubmoss (*Lycopodium annotinum*) and Twinflower (*Linnaea borealis*) are typical representatives.

Corresponds to A in Fremstad.

7. Meadow/Mire/Heath

This class contains bogs, mires, fens and heath, and in the September image; meadows. This is a collective class.

8. Agriculture/open field

This contains open landscape that may be cultured, sward, (re-growing) infields and outfields. In satellite classifications these vegetation types show high spectral values and can be hard to distinguish from rich woodland. This is a collective class.

9. Urban

Contains inhabited areas but can also cover some agricultural lands, and are sometimes hard to distinguish from mires and bogs.

10. Water

Appendix 4 - Tables

Following are the results of the classifications with all classes present.

CLASSIFICATION ACCURACY ASSESSMENT REPORT

Supervised classification of the July image

First is an accuracy assessment with the following class value assignment options.

- Majority Threshold 9
- Use Center Value
- Window size 3

The first supervised classification had 11 classes. In this classification I tried to distinguish between fern and herb dominated Grey Alder – Bird cherry forest, and Rich Swamp woodland.
The classes are: 1 fern and 2 herb Grey Alder, 3 Rich swamp woodland, 4 Aspen, 5 Tall herb, 6 Low herb, 7 Lichen/bryophyte, 8 Meadow/mire/heath, 9 Agriculture/open fields, 10 Urban, 11 water

Table 16. Error matrix from the supervised July classification, with 11 classes.

ERROR MATRIX				
		Reference Data		
Classified Data	Background	Class 1	Class 2	Class 3
Background	0	0	0	0
Class 1	0	8	2	0
Class 2	0	0	2	0
Class 3	0	1	1	0
Class 4	0	18	2	1
Class 5	0	1	1	1
Class 6	0	6	7	2
Class 7	0	5	16	2
Class 8	0	0	2	0
Class 9	0	0	0	0
Class 10	0	0	0	0
Class 11	0	0	0	0
Classified Data	Class 4	Class 5	Class 6	Class 7
Background	0	0	0	0
Class 1	0	3	0	0
Class 2	0	0	0	0

Class 3	2	2	1	0
Class 4	11	5	0	1
Class 5	6	1	0	9
Class 6	1	8	10	4
Class 7	2	4	4	64
Class 8	0	1	0	3
Class 9	0	0	0	0
Class 10	0	0	0	9
Class 11	0	0	0	1
Classified Data	Class 8	Class 9	Class 10	Class 11
Background	0	0	0	0
Class 1	0	3	0	0
Class 2	0	0	0	0
Class 3	0	0	0	0
Class 4	1	3	0	0
Class 5	0	2	0	0
Class 6	0	1	0	0
Class 7	15	9	0	0
Class 8	0	0	0	0
Class 9	0	0	0	0
Class 10	5	3	20	0
Class 11	0	0	0	11

Table 17. Accuracy Totals from the supervised July classification, with 11 classes.

ACCURACY TOTALS					
Class Name	Ref. tot	Class. tot	Nr. corr.	Prod. acc	Users acc
Class 0	0	0	0	---	---
Class 1	39	16	8	20.51%	50.00%
Class 2	33	2	2	6.06%	100.00%
Class 3	6	7	0	0.00%	0.00%
Class 4	22	42	11	50.00%	26.19%
Class 5	24	21	1	4.17%	4.76%
Class 6	15	39	10	66.67%	25.64%
Class 7	91	121	64	70.33%	52.89%
Class 8	21	6	0	0.00%	0.00%
Class 9	21	0	0	---	---
Class 10	20	37	20	100.00%	54.05%
Class 11	11	12	11	100.00%	91.67%
Overall Classification Accuracy =	41.91%				

Table 18. Kappa Statistics from the supervised July classification, with 11 classes.

KAPPA (K^) STATISTICS	
Conditional Kappa for each Category.	
Class Name	Kappa
Class 0	0.0000
Class 1	0.4261
Class 2	1.0000
Class 3	-0.0202
Class 4	0.2041
Class 5	-0.0343
Class 6	0.2177
Class 7	0.3267
Class 8	-0.0745
Class 9	0.0000
Class 10	0.5081
Class 11	0.9135
Overall Kappa Statistics = 0.3079	

Next is a classification with Rich wamp woodland merged with Grey Alder – Bird Cherry Forest. In this classification the classes: 1 Grey Alder, 2 Aspen, 3 Tall herb, 4 Low herb, 5 Lichen/bryophyte, 6 Meadow/mire/heath, 7 Agriculture/ open field, 8 Urban and 9 Water, are present.

First is an accuracy assessment with the following class value assignment options**.**

- Majority Threshold 9
- Use Center Value
- Window size 3

Table 19. Error Matrix from the supervised July classification, with 9 classes

	Reference Data				
Classified Data	Background	Class 1	Class 2	Class 3	Class 4
Background	0	0	0	0	0
Class 1	0	14	2	5	1
Class 2	0	10	9	4	0
Class 3	0	29	7	10	2
Class 4	0	16	1	3	10
Class 5	0	7	0	1	2
Class 6	0	2	0	1	0
Class 7	0	0	0	0	0
Class 8	0	0	0	0	0
Class 9	0	0	0	0	0

Reference Data					
Classified Data	Class 5	Class 6	Class 7	Class 8	Class 9
Background	0	0	0	0	0
Class 1	0	0	3	0	0
Class 2	0	0	3	0	0
Class 3	15	1	3	0	0
Class 4	9	2	9	0	0
Class 5	57	13	0	0	0
Class 6	3	0	0	0	0
Class 7	0	0	0	0	0
Class 8	9	5	3	20	0
Class 9	1	0	0	0	11

Table 20. Accuracy Totals from the supervised July classification, with 9 classes.

Class Name	Ref. tot.	Class. Tot.	Nr. Corr.	Prod. Acc.	Users acc.
Class 0	0	0	0	---	---
Class 1	78	25	14	17.95%	56.00%
Class 2	19	26	9	47.37%	34.62%
Class 3	24	67	10	41.67%	14.93%
Class 4	15	50	10	66.67%	20.00%
Class 5	94	80	57	60.64%	71.25%
Class 6	21	6	0	0.00%	0.00%
Class 7	21	0	0	---	---
Class 8	20	37	20	100.00%	54.05%
Class 9	11	12	11	100.00%	91.67%
Overall Classification Accuracy = 43.23%					

Table 21. Kappa Statistics from the supervised July classification, with 9 classes.

Conditional Kappa for each Category.	
Class Name	Kappa
Class 0	0.0000
Class 1	0.4075
Class 2	0.3024
Class 3	0.0761
Class 4	0.1583
Class 5	0.5832
Class 6	-0.0745
Class 7	0.0000
Class 8	0.5081
Class 9	0.9135
Overall Kappa Statistics = 0.3360	

Another accuracy assessment was carried out on the 9 class image with the following class value assignment options.

- Clear majority
- Discard window
- Window size 3

There were only minor improvements: Overall Classification Accuracy = 43.75 % and Overall Kappa Statistics = 0.3385.

Unsupervised classification of the July image

The classes are: 1 Grey Alder, 2 Aspen, 3 Tall herb, 4 Low herb, 5 Lichen/bryophyte, 6 Meadow/mire/heath, 7 Agriculture/ open field, 8 Urban and 9 Water.

First is an accuracy assessment with the following class value assignment options.

- Majority Threshold 9
- Use Center Value
- Window size 3

Table 22. Error Matrix from the unsupervised July classification, 9 classes

Reference Data					
Classified Data	Background	Class 1	Class 2	Class 3	Class 4
Background	0	0	0	0	0
Class 1	0	50	11	10	5
Class 2	0	5	3	2	0
Class 3	0	14	4	12	0
Class 4	0	1	0	0	10
Class 5	0	8	1	1	0
Class 6	0	0	0	0	0
Class 7	0	0	0	0	0
Class 8	0	0	0	0	0
Class 9	0	0	0	0	0

		Reference Data			
Classified Data	Class 5	Class 6	Class 7	Class 8	Class 9
Background	0	0	0	0	0
Class 1	7	1	5	0	0
Class 2	0	0	1	0	0
Class 3	28	1	12	1	0
Class 4	11	0	0	0	0
Class 5	32	1	0	0	0
Class 6	8	15	0	4	0
Class 7	5	1	3	6	0
Class 8	2	1	0	4	0
Class 9	1	0	0	0	11

Table 23. Accuracy Totals from the unsupervised July classification, 9 classes.

Class Name	Ref. tot.	Class. Tot.	Nr. corr.	Prod. Acc.	Users acc.
Class 0	0	0	0	---	---
Class 1	78	89	50	64.10%	56.18%
Class 2	19	11	3	15.79%	27.27%
Class 3	25	72	12	48.00%	16.67%
Class 4	15	22	10	66.67%	45.45%
Class 5	94	43	32	34.04%	74.42%
Class 6	20	27	15	75.00%	55.56%
Class 7	21	15	3	14.29%	20.00%
Class 8	15	7	4	26.67%	57.14%
Class 9	11	12	11	100.00%	91.67%
Overall Classification Accuracy =	46.98%				

Table 24. Kappa Statistics from the unsupervised July classification, 9 classes.

Conditional Kappa for each Category.	
Class Name	Kappa
Class 0	0.0000
Class 1	0.4064
Class 2	0.2232
Class 3	0.0904
Class 4	0.4256
Class 5	0.6263
Class 6	0.5236
Class 7	0.1394
Class 8	0.5487
Class 9	0.9135
Overall Kappa Statistics = 0.3671	

Another accuracy assessment was carried out with the following class value assignment options.

- Clear majority
- Discard window
- Window size 3

Table 25. Error Matrix from the unsupervised July classification, 9 classes.

	Reference Data				
Classified Data	Background	Class 1	Class 2	Class 3	Class 4
Background	0	0	0	0	0
Class 1	0	54	7	12	6
Class 2	0	4	6	1	0
Class 3	0	14	5	10	0
Class 4	0	1	0	0	9
Class 5	0	5	1	2	0
Class 6	0	0	0	0	0
Class 7	0	0	0	0	0
Class 8	0	0	0	0	0
Class 9	0	0	0	0	0

	Reference Data				
Classified Data	Class 5	Class 6	Class 7	Class 8	Class 9
Background	0	0	0	0	0
Class 1	12	1	5	0	0
Class 2	0	0	1	0	0
Class 3	24	2	11	2	0
Class 4	13	0	0	0	0
Class 5	33	1	0	1	0
Class 6	7	16	0	3	0
Class 7	3	0	4	6	0
Class 8	2	1	0	3	0
Class 9	0	0	0	0	11

Table 26. Accuracy Totals from the unsupervised July classification, 9 classes.

Class Name	Ref. Tot.	Class. Tot	Nr. Corr	Prod. Acc.	Users Acc
Class 0	0	0	0	---	---
Class 1	78	97	54	69.23%	55.67%
Class 2	19	12	6	31.58%	50.00%
Class 3	25	68	10	40.00%	14.71%
Class 4	15	23	9	60.00%	39.13%
Class 5	94	43	33	35.11%	76.74%
Class 6	21	26	16	76.19%	61.54%
Class 7	21	13	4	19.05%	30.77%
Class 8	15	6	3	20.00%	50.00%
Class 9	11	11	11	100.00%	100.00%
Overall Classification Accuracy =	48.83%				

Table 27 Kappa Statistics from the unsupervised July classification, 9 classes.

Conditional Kappa for each Category.	
Class Name	Kappa
Class 0	0.0000
Class 1	0.4002
Class 2	0.4661
Class 3	0.0692
Class 4	0.3592
Class 5	0.6608
Class 6	0.5863
Class 7	0.2554
Class 8	0.4736
Class 9	1.0000
Overall Kappa Statistics = 0.3859	

Unsupervised classification of the September image.

The classes are: 1 Grey Alder, 2 Aspen, 3 Tall herb, 4 Low herb, 5 Lichen/bryophyte, 6 Meadow/bog/heath, 7 Agriculture/ open field, 8 Urban and 9 Water.

First is an accuracy assessment with the following class value assignment options.

- Majority Threshold 9
- Use Center Value
- Window size 3

Table 28. Error Matrix from the unsupervised September classification, 9 classes.

	Reference Data				
Classified Data	Background	Class 1	Class 2	Class 3	Class 4
Background	0	0	0	0	0
Class 1	0	23	1	6	4
Class 2	0	1	3	2	0
Class 3	0	14	6	6	3
Class 4	0	0	1	0	0
Class 5	0	2	0	0	0
Class 6	0	0	0	0	0
Class 7	0	1	0	1	0
Class 8	0	0	0	0	0
Class 9	0	0	0	0	0

Reference Data					
Classified Data	Class 5	Class 6	Class 7	Class 8	Class 9
Background	0	0	0	0	0
Class 1	4	1	1	0	0
Class 2	0	0	0	0	0
Class 3	6	3	1	1	0
Class 4	1	0	2	0	0
Class 5	18	0	0	0	0
Class 6	1	0	1	1	0
Class 7	0	0	3	1	0
Class 8	0	0	0	1	0
Class 9	0	0	0	0	2

Table 29. Accuracy Totals from the unsupervised September classification, 9 classes.

Class Name	Ref. tot.	Class. Tot.	Nr. Tot.	Prod. Acc.	Users acc.
Class 0	0	0	0	---	---
Class 1	41	40	23	56.10%	57.50%
Class 2	11	6	3	27.27%	50.00%
Class 3	15	39	6	40.00%	15.38%
Class 4	6	4	0	0.00%	0.00%
Class 5	30	20	18	60.00%	90.00%
Class 6	4	3	0	0.00%	0.00%
Class 7	8	6	3	37.50%	50.00%
Class 8	4	1	1	25.00%	100.00%
Class 9	2	2	2	100.00%	100.00%
Overall Classification Accuracy =	46.28%				

Table 30. Kappa Statistics from the unsupervised September classification, 9 classes.

Conditional Kappa for each Category.	
Class Name	Kappa
Class 0	0.0000
Class 1	0.3572
Class 2	0.4500
Class 3	0.0341
Class 4	-0.0522
Class 5	0.8670
Class 6	-0.0342
Class 7	0.4646
Class 8	1.0000
Class 9	1.0000
Overall Kappa Statistics = 0.3254	

Another accuracy assessment was carried out with the following class value assignment options.

- Clear majority
- Discard window
- Window size 3

The results of this classification were slightly worse:
Overall Classification Accuracy = 46.15 % and Overall Kappa Statistics = 0.3291

Appendix 5 - Models

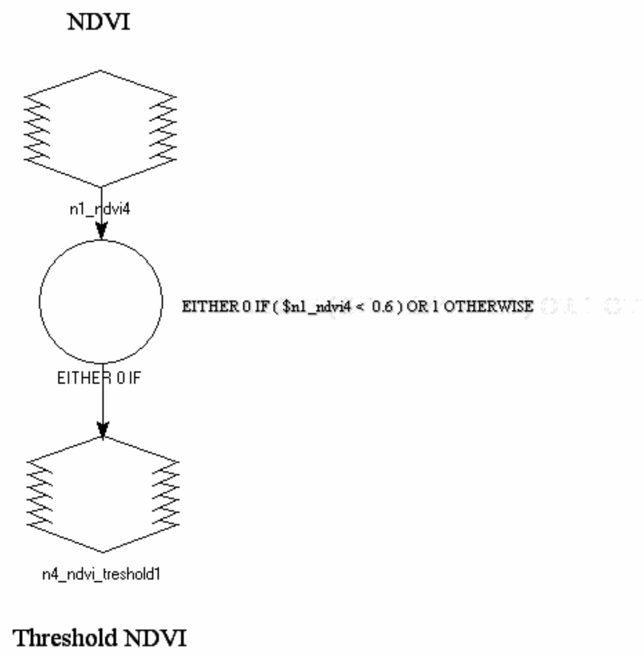

Figure 25. The model that was used to make a threshold NDVI.

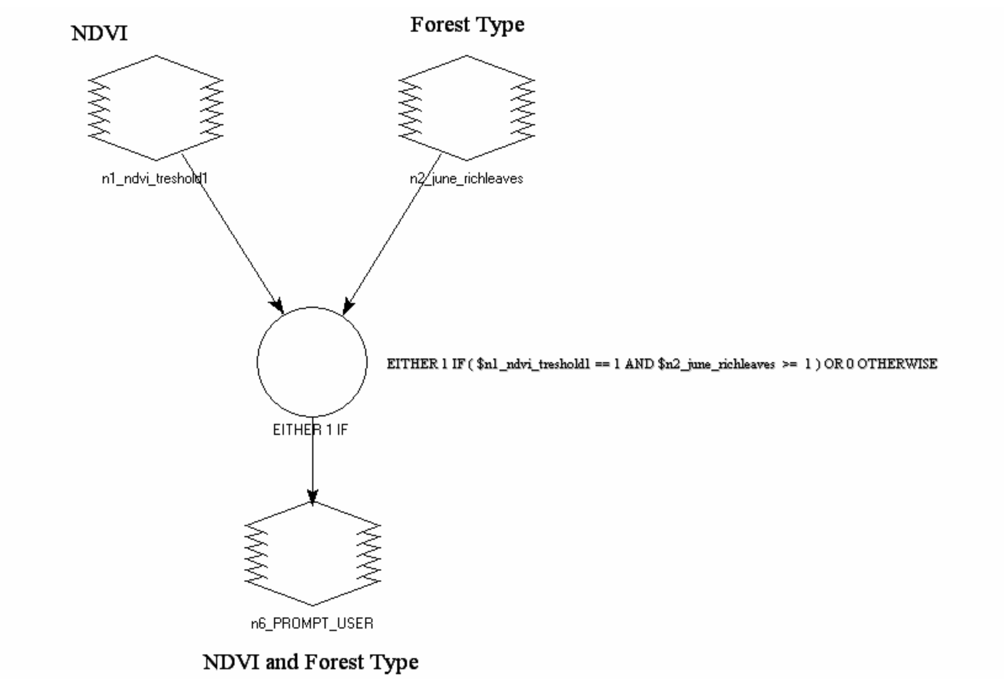

Figure 26. Model used to make a composite of the Threshold NDVI and the unsupervised July classification with 4 classes.

Appendix 6 - Glossary

Based on (Lillesand et al., 2000; Heywood et al., 2002; Clarke, 2003; Pettorelli et al., 2005)

Accuracy: The validity of data measured with respect to an independent source of higher reliability and precision.

Arc: A line that begins and ends at a topologically significant location, represented as a set of sequential points.

Arc/Info: A GIS software package developed by the Environmental Systems Research Institute (ESRI).

Base layer or map: A GIS data layer of reference information, such as topography, road network or streams, to which all other layers are referenced geometrically

Datum: A base reference level for the third dimension of elevation for the earth's surface. A datum can depend on the ellipsoid, the earth model, and the definition of sea level.

DEM (Digital elevation model). A data format for digital topography, containing an array of terrain elevation measurements.

GIS: A system of hardware, software, data, people, organizations, and institutional arrangements for collecting, storing, analyzing, and disseminating information about the earth (one of many definitions).

GPS (Global Positioning System): An operational, U.S. Air Force-funded system of satellites in orbits that allow their use by a receiver to decode time signals and convert the signals from several satellites to a position on the earth's surface.

IKONOS: High resolution satellite from Space Imaging Inc. The sensor has a 1x1 meter panchromatic band and four multispectral visible and near-infrared bands at 4x4 meter spatial resolution. Has a sun-synchronous orbit and frequent revisit capability.

Landsat 7 Enhanced Thematic Mapper Plus: Satellite with 8 bands, 6 of which has a 30×30 m spatial resolution. The thermal infrared band (band 6) has a 60×60 m resolution. In addition is the 15×15 m panchromatic band. The satellite is sun-synchronous and has a revisit time of 16 days.

Map projection: A depiction of the earth's three-dimensional structure on a flat map.

Mask: A map layer intended to eliminate or exclude areas not needed for mapping and analysis.

Matrix: A table of numbers with a given number of rows and columns.

Mosaicing: The GIS or digital map equivalent of matching multiple paper maps along their edges. Features that continue over the edge must be "zipped" together and the edge dissolved. A new geographic extent for the map usually has to be cut or clipped out of the mosaic. To permit mosaicing, maps must be on the same projection, datum, ellipsoid, and scale, and show features captured at the same equivalent scale.

NDVI (Normalized Difference Vegetation Index): A satellite based vegetation index that correlates strongly with aboveground net primary productivity. Uses red and near infrared reflectance values.

NDWI (Normalized Difference Water Index): A vegetation index for remote sensing of vegetation liquid water, using near infrared and short wave infrared reflectance values.

Node: The end of an arc.

Pixel: The smallest unit of resolution on a display, often used to display one grid cell at the highest display resolution.

Point: A zero-dimensional map feature, such as a single elevation mark as specified by at least two coordinates.

Polygon: A many-sided area feature consisting of a ring and an interior. An example is a lake on the map.

QuickBird: High resolution satellite from EarthWatch Inc. Non.sun-synchronous orbit, with a revisit time from 1 to 5 days. Has a 0.61×0.61 m panchromatic band and four visible/near-infrared bands at 2.44×2.44 m spatial resolution.

Raster: A data structure for maps based on grid cells.

Remotely sensed data: Data collected by a sensor that is not in direct contact with the area being mapped. Can be active or passive.

Sample: A subset of a population selected for measurement.

Scale: The geographic property of being reduced by the representative fraction. Scale is usually depicted on a map or can be calculated from features of known size.

Spatial: Anything pertaining to the concepts of space, pace and location.

Spatial data: Data that have some form of spatial or geographical reference that enables them to be located in two- or three-dimensional space.

SPOT (Systeme Proprietaire pour l'Observation de la Terre): A French remote sensing satellite system with 10- and 20-meter resolution and stereo capability.

Subsetting: Extracting a part of a data set.

Supervised classification: The, user supervised/controlled, grouping of pixels by their numerical spectral value.

Thresholding: Is used to segment an image into two classes – one for those pixels having values below an analyst-defined level, and one for values above this value.

Topology: The property that describes adjacency and connectivity of features. A topological data structure encodes topology with the geocoded features.

Transverse: A map projection in which the axis of the map is aligned from pole to pole rather than along the equator.

Unsupervised classification: The grouping of pixels by their numerical spectral characteristics without the intervention of direct human guidance.

UTM (Universal Transverse Mercator): A standardized coordinate system based on the metric system and a division of the earth into sixty 6-degree-wide zones. Each zone is projected onto a transverse Mercator projection, and the coordinate origins are located systematically.

Vector: A map data structure using the point or node and the connecting segment as the basic building block for representing geographic features.

Vectorization: The process of converting data from raster to vector format.

WGS84 (World Geodetic Reference System of 1984): A common datum and reference ellipsoid for hand held GPS receivers.

Zone: The region over which the coordinates relate with respect to a single origin.

A line is a dot that went for a walk.

~ Paul Klee